Agricultural Water Management 334 (2026) 110700

Contents lists available at ScienceDirect

Agricultural Water Management

journal homepage: www.elsevier.com/locate/agwat

Multi-scale assessment of irrigation water use and supply in the Amibara Irrigation Scheme, Ethiopia using Landsat-derived evapotranspiration and field data

Kirubel Mekonnen[a,*], Mulugeta Tadesse[a], Naga Manohar Velpuri[b], Mohammed Abdella[a], Mengistu Dessalegn[a], Mansoor Leh[b], Komlavi Akpoti[c], Afua Owusu[c], Ashenafi Likessa[d], Abdulkarim Seid[a]

[a] International Water Management Institute, Addis Ababa, Ethiopia
[b] International Water Management Institute, Colombo, Sri Lanka
[c] International Water Management Institute, Accra, Ghana
[d] Ministry of Irrigation and Lowlands, Addis Ababa, Ethiopia

ARTICLE INFO

Keywords:
Irrigation Water Use
Irrigation Water Supply
Crop Type, Blue ET
Multi-Scales
Irrigation Performance

ABSTRACT

Accurate estimation of irrigation water use and supply is essential for effective irrigation management, yet irrigation withdrawals remain largely unmetered and unreported in many schemes. This study applied a remote sensing–based approach to quantify irrigation water use and supply in the Amibara Irrigation Scheme, Ethiopia. The irrigation component of crop evapotranspiration (Blue ET) was partitioned from a high-resolution Landsat-based ETa product using the Water Accounting Plus (WA+) framework. Blue ET estimates were then integrated with irrigation efficiency parameters to derive remote sensing–based irrigation supply (RbIS) at block, canal and scheme scales. Crop type maps for 2010 and 2024 and a digitized irrigation layout provided the spatial basis for assessing irrigation performance using relative evapotranspiration (RET) and relative irrigation supply (RIS) metrics. Crop mapping revealed a substantial decline in the gravity-fed irrigated area from 9941 ha in 2010 to 4532 ha in 2024. RbIS showed reasonable agreement with reported irrigation supply in 2010 ($R^2 = 0.58$) and measured supply in 2024 ($R^2 = 0.77$), although supply was consistently underestimated. The extent of irrigation water deficits increased between 2010 and 2024, with the proportion of cotton blocks experiencing water deficits rising from 40% to 67%. Key informant interviews and focus group discussions corroborated the observed irrigation water deficits in 2024, supporting the remote sensing–based assessment. Moreover, RET and RIS revealed spatial variability in irrigation performance across irrigation canals, suggesting potential under and over-supply of irrigation. Overall, the proposed approach provides a scalable framework for assessing irrigation water use and supply in data-scarce irrigation schemes.

1. Introduction

Accurate estimation of irrigation water use and supply is essential for effective water management and for promoting evidence-based, equitable, and efficient water allocation (Ji et al., 2025; Muturi et al., 2025; Zipper et al., 2024). However, obtaining reliable measurements remains a persistent challenge, particularly in regions where irrigation withdrawals are neither metered nor consistently reported (OECD, 2015). Even when the physical locations of abstractions are known, the installation and maintenance of in-situ metering devices face significant technical, financial, and political constraints (Foster et al., 2020; Ji et al., 2025; Rinaudo et al., 2016). These challenges are especially pronounced in many African irrigation schemes, where limited monitoring infrastructure constrains reliable assessment of irrigation water use and supply.

Remote sensing provides an opportunity to complement limited ground-based monitoring by enabling spatially explicit estimation of agricultural water use across large geographic areas (Mekonnen et al., 2024; Zhang et al., 2022; Zwart and Leclert, 2010). Most remote sensing–based approaches rely on actual evapotranspiration (ET) to

* Corresponding author.
E-mail address: k.gebreyesus@cgiar.org (K. Mekonnen).

https://doi.org/10.1016/j.agwat.2026.110700
Received 28 March 2026; Received in revised form 8 August 2026; Accepted 13 August 2026
Available online 17 August 2026

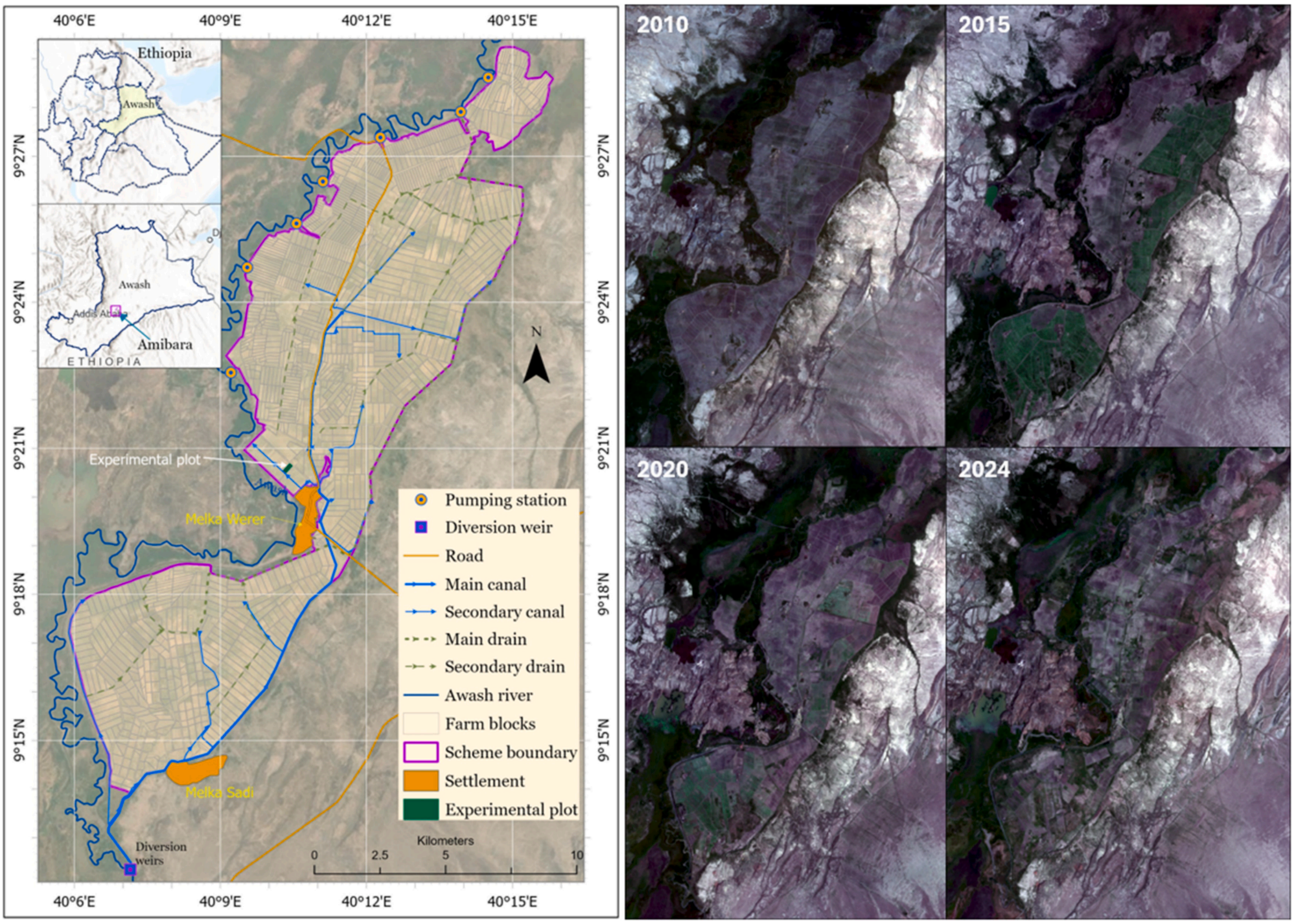

Fig. 1. Location of the Amibara Irrigation Scheme and annual geomedian Landsat composites for the single tile covering the study *area, showing* the progression of Prosopis juliflora development 20*10*–2024.

quantify crop water consumption, making ET a key variable for irrigation monitoring. Advances in satellite observations and ET modelling have led to the development of several operational ET products, including WaPOR (FAO, 2020), MOD16 ET (Mu et al., 2011), SSEBop (Senay et al., 2013; Senay et al.,2020), and GLEAM (Miralles et al., 2011). These products provide long-term spatial explicit datasets that have been widely applied for agricultural water-use assessment and irrigation management.

Despite their potential, most globally available remotely sensed ET datasets face two key limitations that constrain their use in operational irrigation management. First, their coarse spatial resolution limits the ability to assess water use at the plot or field scale, where irrigation decisions are made. Second, uncertainties associated with the underlying ET algorithms, input data quality, and sensor characteristics can introduce biases into ET estimates (Dile et al., 2020; Mekonnen et al., 2022; Tran et al., 2023). These uncertainties underscore the need for validating remote sensing–based estimates of irrigation water use against reliable ground observations to assess their accuracy and ensure their suitability for operational applications. However, such validation is further complicated by the limited availability of independent observations at operational scales.

Several studies have evaluated remote sensing-based irrigation water use estimates against ground-based observations (Ji et al., 2025; Zipper et al., 2024). For example, Ji et al. (2025) compared irrigation water use derived from high-resolution ET datasets with the reported groundwater withdrawal volumes, highlighting the potential of the remotely sensed ET estimates for operational water management. Similarly, Zipper et al. (2024) assessed irrigation water use at field, water-right, and regional scales, underscoring the importance of scale when validating remote-sensing ET products. While these studies offer valuable insights into consumptive use, direct comparisons between ET-based water use and reported irrigation supply remain challenging because the two variables represent different components of the water balance. Remote sensing–derived ET represents the actual water consumed by crops, whereas reported irrigation supply reflects the gross volume of water diverted or delivered to an irrigation scheme, including conveyance and other non-consumptive losses. As a result, direct comparison between these variables is inherently challenging. Additional uncertainties arise from inaccuracies in reported supply records and from spatial and temporal mismatches, since ET is typically estimated at pixel scale, while irrigation supply is commonly reported at canal or scheme levels.

To address these challenges, this study integrates remotely sensed estimates of consumptive water use with irrigation efficiency information to reconstruct irrigation water supply, which is then evaluated against available canal- and scheme-level water delivery records. Beyond validation, this study provides a spatially explicit assessment of irrigation water use and supply across scheme, canal, and irrigation-block scales. This multi-scale assessment enables the identification of spatial variations in irrigation performance and water distribution that may not be apparent from scheme-level analyses alone, thereby complementing previous studies (e.g., Abera et al., 2019; Asres, 2016; Bashe et al., 2023; Ji et al., 2025; Mekonnen et al., 2024; Yadeta et al., 2022; Zipper et al., 2024) that have mainly focused on scheme-scale water use assessments.

Table 1
Dataset used for this study.

Class	Dataset	Temporal/spatial (m) resolution	Data availability -period	Source
In situ	Climate data	Daily	2001–2024	Melka Werer Agricultural Research Center
	Discharge data	Daily	1991–2014	Ministry of Water and Energy
	Crop coefficient (kc) including planting and harvesting dates for the major crops	Seasonal	-	Melka Werer Agricultural Research Center
	Irrigation water supply	Seasonal	2010,2024/25	IWMI
	Soil moisture before and after an irrigation event	-	2024/25	IWMI
	Reported water withdrawal data in volume	Monthly (July-September)	2010–2011	Awash Basin Authority
Remote sensing	CHIRPS rainfall data (CHIRPS v2)	Daily/5000	2010–2024	(Funk et al., 2015)
	High resolution SSBop ETa from Landsat imagery	Monthly/30	2010–2024/25	(Senay et al., 2022)
	High resolution land cover	Yearly/100	2010–2024	IWMI
	WaPOR reference ETo	Decadal/100/	2010–2024	FAO (2020)
	Saturated soil water content	0.0025/Static		Simons et al., (2020)
	Net primary production (NPP)-MOD 17	0.005/8-day	2010–2024	Zhao et al. (2005)
	Gross primary production (GPP) MOD 17	0.005/8-day	2010–2024	Zhao et al. (2005)
	Leaf area index (MODIS 15)	0.005/8-day	2010–2024	Myneni et al. (2002)
	Others remote sensing inputs for WA + (annex 1)			-
	Digital irrigation layout			IWMI

Building on this multi-scale framework, the present study aims to: (i) estimate spatially explicit irrigation water use and supply across scheme, canal, and block, scales in the Amibara Irrigation Scheme; (ii) compute key irrigation performance indicators using remote sensing-based water-use estimates; and (iii) examine the potential of alternative water management scenarios to improve irrigation water use. By generating a comprehensive multi-scale evaluation of irrigation water use and supply, this study provides an analytical foundation for evidence-based irrigation water management. The findings support the development of targeted interventions to improve irrigation performance and contribute to broader national objectives related to irrigation system rehabilitation and long-term water security.

2. Materials and methods

2.1. Study area

The Amibara irrigation scheme is located in the Afar Regional State of Ethiopia, specifically in Amibara Woreda (district), along the right bank of the Awash River's alluvial plain. The scheme receives its water from the Awash River through a diversion weir located upstream of Melaka Sedi town, as well as from several pumping stations located along the river downstream of Melka Werer town. Geographically, this large-scale irrigation scheme is situated between latitude 9.231°N and 9.487°N, and longitude 40.098°E and 40.264°E (Fig. 1).

Initiated in 1978 and completed in 1984, the Amibara irrigation scheme covers approximately 15,000 ha, of which 10,300 ha are irrigated via gravity flow from the diversion weir upstream of Melka Sedi, while the remaining area is served by multiple downstream pumping stations (World Bank, 1990). The dominant crop in the scheme is cotton, and the irrigation method used is furrow irrigation. The topography of the region is predominantly flat to gently sloping (0.5–2%), with an average elevation of 740 m above mean sea level, making it suitable for large-scale agricultural development. The vegetation is dominated by the invasive tree species *Prosopis juliflora,* reclassified as *Netluma julifora*, which was introduced in the early 1980s to combat desertification (Shiferaw et al., 2021). Well-adapted to the semi-arid climate, this species has spread aggressively and become ecologically disruptive, negatively affecting native biodiversity and agricultural productivity (Shiferaw et al., 2021; Zeray et al., 2017).

The rainfall pattern of the study area is characterized by a bimodal rainfall pattern, with a long rainy season from July to September and a shorter rainy season from March to May. Temperatures are generally high throughout the year, with maximum daytime temperatures reaching up to 37 °C in June, while minimum temperatures decline to around 15 °C in December.

2.2. Data

All the datasets used in this study are summarized in Table 1. Both in situ and remotely sensed datasets were used for crop type mapping, irrigation layout digitization, and estimating irrigation water use and supply.

2.2.1. In situ data

In situ data were collected from multiple sources. These datasets included daily climatic data (rainfall and pan evaporation), river discharge records, irrigation water supply measurements, soil moisture observations, and reported irrigation water withdrawal data.

Daily climate data, including rainfall and pan evaporation, were obtained from the Melka Werer Agricultural Research Center, located in the Amibara Irrigation Scheme, Afar Regional State, Ethiopia. The observed rainfall data were used to validate multiple remotely sensed rainfall products, following the approach of Mekonnen et al. (2023), after which the most suitable product was selected for further analysis. Pan evaporation measurements were used to estimate reference evapotranspiration (ETo), which served as input for estimating crop water requirements.

Daily discharge data were sourced from the Ministry of Water and Energy and used to estimate the long-term monthly dependable flow at the scheme diversion site. Dependable flow refers to the river discharge equaled or exceeded at a given probability of exceedance and represents the amount of water that can be reliably diverted for irrigation. In this study, the 80% dependable flow (Q80) was adopted, consistent with the design standard used for the original diversion weir. The estimated monthly Q80 flow was then compared with the weir's design diversion capacity (13.2 m^3 s^{-1}) to evaluate whether the available river flow can reliably meet the scheme's original design water demand. This assessment is particularly important because the irrigation scheme was constructed more than three decades ago, and current hydrological conditions may differ from those assumed in the original design.

Irrigation water supply was monitored from December 2024 to March 2025 in a 6-ha experimental plot (Fig. 1), as observed irrigation water supply data have not been available for the scheme since 2011. The experimental plot was located in the central part of the scheme where cotton is the predominant crop and furrow irrigation is the prevailing irrigation method. We assumed that this plot was representative of the dominant irrigation practices within the scheme. Irrigation water delivered to the plot was measured using a Parshall flume installed at the field inlet. A total of 43 irrigation applications were monitored. The

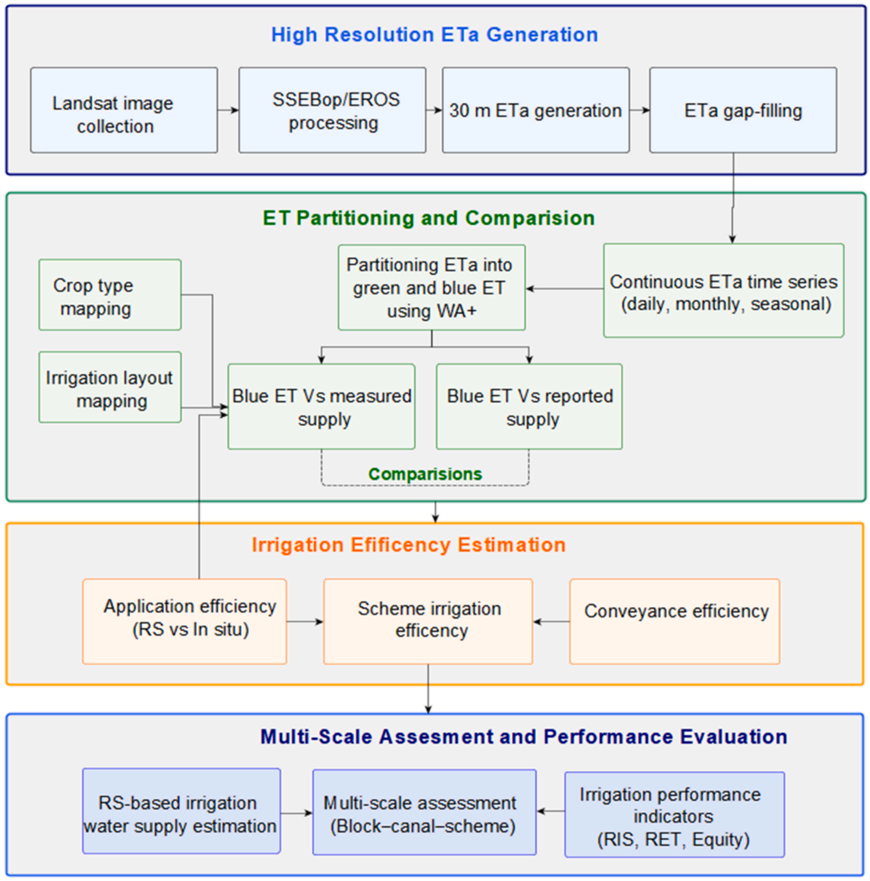

Fig. 2. Overall workflow of the study. Blue ET refers to the irrigation-derived component of actual evapotranspiration, while green ET represents the rainfall-derived component. WA + denotes the Water Accounting Plus framework. RIS and RET refer to Relative Irrigation Supply and Relative Evapotranspiration, respectively. RS refers to remote sensing.

spatial coordinates of the irrigated areas were also recorded, as individual irrigation events covered only portions of the 6-ha experimental plot. These irrigation water supply data were used to evaluate the remote sensing–based irrigation water supply estimates and derive irrigation application efficiency. In addition, reported irrigation supply data obtained from the former Awash Basin Authority were used to further validate the remote sensing-based irrigation supply estimates for 2010.

In situ soil moisture measurements were also conducted within the experimental plot and used as input to estimate irrigation application efficiency. Root-zone water storage was determined from soil samples collected before irrigation and 48 h after irrigation. The 48-hour interval was selected because the study area is predominantly characterized by clay soils, which have low drainage rates following irrigation. This interval allows excess water to drain and soil moisture to stabilize closer to field capacity, thereby providing a more representative measure of root-zone water storage (Nasta et al., 2023). Soil moisture was determined using the gravimetric method from composite samples collected from the 0–90 cm soil profile at five locations distributed along the plot diagonals. Gravimetric moisture content was calculated on a mass basis and converted to an equivalent water depth using soil bulk density and effective root-zone depth.

2.2.2. *Remote sensing datasets*

Several remote sensing datasets were used in this study. Landsat 5, 7, 8, and 9 imagery, acquired from the USGS earth explorer (EarthExplorer), were used to create high-resolution evapotranspiration (ETa) estimates for the period 2010–2025 and to develop crop type maps. In addition, multiple remotely sensed datasets were integrated into the Water Accounting Plus (WA+) framework to partition actual evapotranspiration into green ET (rainfall-based water use) and blue ET (irrigation-based water use) using a soil moisture balance approach. A summary of the remote sensing datasets used in the WA + analysis is provided in Annex 1.

2.3. *Methods*

The overall workflow of this study is presented in Fig. 2. The workflow consists of four main components: (i) generation of high-resolution ETa, (ii) partitioning of ETa into green and blue ET and comparison with irrigation water application data, (iii) estimation of representative irrigation efficiency, and (iv) multi-scale irrigation performance assessment.

2.3.1. *Creating a high-resolution ETa dataset*

We created a high-resolution (30 m) ETa product from Landsat imagery to assess field-scale irrigation water use. The Landsat scenes were processed through the EROS Science Processing Architecture (ESPA) on-demand platform, which applies the Simplified Surface Energy Balance Operational (SSEBop) algorithm (Senay et al., 2016,2020, 2022). SSEBop integrates multispectral remote sensing data with meteorological inputs to estimate ETa, as described in Eqs. 1–2:

$$ETa = ETf * K * ETo \tag{1}$$

$$ETf = 1 - \gamma s(Ts - Tc) \tag{2}$$

Where ETf is the evapotranspiration fraction, ETo is the reference evapotranspiration for a grass surface (mm/day), and k is a scaling factor. ETf is derived from the relationship between surface temperature (Ts) and the cold (Tc) and hot (Th) boundary temperatures. Detailed descriptions of the SSEBop algorithm are provided in earlier studies (e.g., de Andrade et al., 2021; Senay et al., 2013). The step-by-step procedure for estimating high-resolution ETa using the SSEBop algorithm through the Landsat on-demand processing platform is provided in Annex 2.

In this study, Landsat images (Path 167 and Row 054) with cloud cover of up to 52% were acquired for the period 2010–2025, resulting in a total of 524 scenes. These images were processed to generate spatially distributed ETa estimates. However, persistent cloud contamination introduced substantial spatial gaps in the ETa datasets. To address this limitation, a two-step gap-filling procedure was applied separately for each calendar month. First, all available ETa rasters for a given month across the study period were aggregated to generate a long-term pixel-wise monthly median composite. This composite served as a robust month-specific reference, reducing the influence of cloud-related anomalies while preserving the seasonal characteristics of ETa. Second, any remaining gaps in the monthly median composite were filled using a focal median filter within a moving spatial window. The window size was determined iteratively to ensure complete gap filling while preserving local spatial variability and minimizing excessive smoothing. Finally, cloud-contaminated pixels in each monthly ETa raster were replaced with values from the reconstructed monthly median composite, resulting in spatially complete ETa datasets for subsequent analyses. Similar focal-statistics approaches have been widely applied to reconstruct remote sensing products such as evapotranspiration, land surface temperature, and energy balance datasets (Senkondo et al., 2019; Siabi et al., 2022; Wang et al., 2022).

2.3.2. *Partitioning of Blue ET from high-resolution ETa*

Several approaches have been proposed for estimating blue ET: the soil water balance model (Karimi et al., 2013), the Budyko framework (De Boer, 2016), the coupled Energy balance-Water balance approach (Velpuri and Senay, 2017) and the Van Eekelen method (van Eekelen et al., 2015). In this study, a simplified soil water balance model embedded within WA + was applied to partition total ETa into green and blue ET. A detailed description of the WA + framework is available in previous studies (e.g., Dembélé et al., 2023; Karimi et al., 2013; Mekonnen et al., 2026; Owusu et al., 2024)

Within the WA + framework, green ET refers to evapotranspiration derived from rainfall stored in the root zone, whereas blue ET refers to evapotranspiration sustained by water supplied through managed sources, including rivers, reservoirs, lakes, and groundwater (Mekonnen et al.,2026). The partitioning is based on a monthly root-zone soil moisture balance that accounts for antecedent soil moisture, effective precipitation, actual evapotranspiration, percolation losses, and surface runoff. Rainfall-derived soil moisture is assumed to satisfy evapotranspiration demand first, and any remaining water demand that cannot be met from rainfall is attributed to irrigation and classified as blue ET. Consequently, green ET and blue ET together account for total actual evapotranspiration.

Blue ET was estimated using the soil moisture accounting procedure embedded within WA + , as described in Eqs. (3–5):

$$ET_{blue} = \begin{cases} 0, & if\ (SM_t \geq 0) \\ (SM_t \times -1) & if\ (SM_t < 0) \end{cases} \tag{3}$$

$$ET_{green} = \begin{cases} ET_a & if\ (SM_t > ET_a) \\ ET_a - ET_{blue} & if\ (SM_t < ET_a) \end{cases} \tag{4}$$

$$SM_t = SM_{t-1} + (P - I)_t - (ET_a - I)_t - QP_t - QS_r \tag{5}$$

Where SM_t is the soil moisture at time t, calculated using a soil water balance approach that incorporates the previous day's soil moisture (SM_{t-1}), effective precipitation (defined as precipitation minus interception, (P - I), actual evapotranspiration (ETa), percolation losses (QP_t), and surface runoff (QS_r). ET_{green} represents the portion of ETa derived from rainfall stored in the root zone. In rainfed landscapes, SM_t is zero or positive, but it becomes negative when ETa exceeds the available soil moisture, indicating the contribution of additional water sources (i.e., irrigation), which is attributed to Blue ET.

Accurate partitioning of ETa into green ET and blue ET was essential because the study period coincides with the main rainy season, when crops received water from both rainfall and supplementary irrigation. Thus, total ETa reflected the combined contributions of these two water sources and could not be directly attributed to irrigation. Partitioning ETa into green and blue components allowed the irrigation-derived water use to be isolated from rainfall-derived evapotranspiration, thereby improving the estimation of irrigation water use and supply from remotely sensed ETa.

2.3.3. *Irrigation layout and crop type mapping*

An accurate irrigation layout map is essential for evaluating scheme performance across multiple spatial scales. However, no complete digital layout of the study area was available. To address this gap, the irrigation layout was reconstructed by integrating high-resolution imagery with scanned legacy blueprints. The canal network and field boundaries were digitized, and the resulting layout map was verified in consultation with the enterprise managing a large portion of the scheme.

To support the analysis of irrigation water use, crop type maps were developed for 2010 and 2024. These years were selected to represent two contrasting operational states of the Amibara irrigation scheme. The year 2010 corresponds to a period when the scheme was operating closer to its original design capacity, whereas 2024 represents the current condition following major disturbances, including the 2020 floods and the expansion of invasive tree species, *Prosopis juliflora.* Crop types were identified through visual interpretation of Landsat and Sentinel−2 imagery, supported by high-resolution imagery from Google Earth and field survey.

For the 2010 map, crop identification was facilitated by the predominantly monocropped agricultural system, in which cotton was the dominant crop. Cotton fields could be differentiated relatively clearly from the limited number of other land-cover classes, including settlements, trees, and shrubs, based on their spatial configuration, field characteristics, and spectral appearance. Land-use and crop maps for 2024 were produced through manual visual interpretation of satellite imagery rather than automated image classification. The interpretation integrated multi-temporal Sentinel−2 imagery, seasonal NDVI profiles, field boundaries, and expert knowledge of the agricultural production system. Cotton fields were independently verified against farm management logbooks containing field identification numbers and corresponding crop records. Permanent land-cover classes, including settlements, flooded areas, trees, shrubs, and experimental plots of the research center, were identified based on their stable spatial characteristics and contextual information. Other crop types, including vegetables, date palms, and mixed crops, were distinguished based on their seasonal spectral responses, field characteristics, and visual interpretation of multi-temporal imagery.

Efforts were also made to identify unauthorized irrigated areas, defined as (i) irrigated lands located outside the scheme boundaries and (ii) irrigated lands within the scheme boundaries that abstract water directly from the main canal without authorization. These data were used to estimate the volume of unauthorized abstraction from the main canal.

2.3.4. *Estimation of irrigation efficiency*

Field application and conveyance efficiencies were estimated from in situ observations and used to derive the overall irrigation efficiency of the scheme. These efficiencies were determined by integrating soil moisture measurements, canal discharge measurements, and continuous monitoring of irrigation water applied to a representative experimental

Table 2
Summary of irrigation performance indicators used in this study.

Indicator	Performance dimension	Definition	Formula	Class	Interpretation	Reference
Equity	Water distribution uniformity	Measures the uniformity of water consumption across blocks or users within the irrigation scheme	$Equity = \frac{Sd(ETa)}{Mean(ETa)}$	Good: CV ≤ 10% Fair: 10% < CV ≤ 25% Poor: CV > 25%	Lower values indicate more equitable water distribution; higher values reflect uneven /poor water distribution	(Chukalla et al., 2022; Karimi et al., 2019)
RET (Relative Evapotranspiration)	Crop water adequacy	Ratio of actual evapotranspiration to crop water requirement over the irrigation season	$RET = \frac{ETa}{ETc}$	Good: 0.8 < RET ≤ 1.0 Acceptable: 0.68 < RET ≤ 0.8 Poor: RET ≤ 0.68	Identifies areas experiencing water stress or adequate crop water use	(Karimi et al., 2019; Poudel et al., 2021)
RIS (Relative Irrigation Supply)	Supply–demand balance	Ratio of irrigation water supplied to net irrigation demand	$RIS = \frac{RbIS}{IrrD}$	Deficit: RIS < 0.99 Optimal: 0.99 ≤ RIS ≤ 1.01 Excess: RIS > 1.01	Higher values indicate oversupply, whereas lower values indicate undersupply.	(Usman et al., 2020;Haj-Amor et al. 2018)

Notes:$ET_a$is actual evapotranspiration derived from high-resolution remote sensing; $ET_c$is crop water requirement estimated from reference evapotranspiration and crop coefficients; *RbIS*is remote sensing-based irrigation supply derived from blue ET; *IrrD*is irrigation demand computed as ET_cminus effective rainfall. Effective rainfall was estimated using the FAO-recommended USDA Soil Conservation Service method.

plot. However, continuous monitoring of canal flow and soil moisture across the entire Amibara Irrigation Scheme was not feasible because of logistical constraints, the absence of functional flow metering structures, and the large spatial extent of the scheme. Consequently, the available soil moisture and canal discharge measurements were used to estimate field application efficiency (Eq. 6) and conveyance efficiency (Eq. 7), respectively.

Cotton cultivated under furrow irrigation is the dominant cropping system across the scheme, and irrigation practices are relatively uniform among irrigation blocks. Given this, the field application efficiency derived from the experimental plot and the conveyance efficiency estimated from canal measurements were assumed to be representative of the average irrigation efficiency of the scheme. This assumption enabled the estimation of scheme-wide irrigation water supply in the absence of spatially distributed measurements of irrigation efficiency.

Application efficiency (*Ea*- Eq. 6) was calculated as the ratio of the volume of irrigation water stored within the crop root zone (*WSr*) to the total volume of water applied to the experimental plot (*WA*):

$$Ea = \frac{WSr}{WA} \tag{6}$$

where *WSr* represents water stored in the root zone and *WA* denotes the irrigation water applied to the plot (Fig. 2). The application efficiency derived from in situ observations (Eq. 6) was compared with the remote sensing–derived efficiency, which was estimated using blue ET and the measured irrigation water supply.

Conveyance efficiency (*Ec*- Eq. 7) was estimated from discharge measurements conducted along selected reaches of the main and secondary canals using a current meter (Fig. 2), and computed as:

$$Ec = \frac{Vf}{Vt} \tag{7}$$

where Ec is water conveyance efficiency (%), Vf is the volume of irrigation water at the downstream reach, and Vt is the volume of irrigation water at the upstream reach. Efficiency values obtained at different canal sections were averaged to estimate system-level conveyance efficiency.

The overall irrigation efficiency of the scheme was estimated as the product of application ,conveyance, distribution efficiencies. For the 2024/2025 irrigation season, the average field application efficiency measured at the experimental plot was 0.48, compared with 0.45 estimated using the remote sensing–based approach, indicating good agreement between the two estimates. Given the availability of direct field observations, the measured application efficiency (0.48) was adopted for subsequent analysis. The average conveyance efficiency was 0.82 and distribution efficiency (E_d) was assumed to be 0.82. Based on these values, the overall irrigation efficiency of the scheme was estimated at 32%. This value is lower than the original design efficiency of 49% (Halcrow, 1983). For the 2010 irrigation season, an overall irrigation efficiency of 43%, reported by Sahle (2009), was adopted.

2.3.5. Estimation of remote sensing-based irrigation water supply (RbIS)

The remote sensing-based irrigation water supply (RbIS) was estimated by dividing blue ET with irrigation efficiency. RbIS was calculated using Eq. (8), following the approach proposed by Ji et al. (2025).

$$RbIS = \frac{Blue\ ET}{IE} \tag{8}$$

where RbIS is a remote sensing-based irrigation water supply, and IE is overall irrigation efficiency.

Monthly RbIS estimates were generated for 2010 and 2024. Since RbIS estimation is sensitive to irrigation efficiency, a representative scheme-wide irrigation efficiency value was selected for each study year and applied uniformly across the scheme. This approach was necessary because spatially distributed data on irrigation water withdrawals and irrigation efficiency were unavailable. It further assumes that irrigation performance does not vary substantially among irrigation blocks. This assumption is considered reasonable for the Amibara Irrigation Scheme, where furrow irrigation is the dominant irrigation method, cotton occupies most of the cultivated area, and irrigation management practices are generally similar across the scheme. Nevertheless, the use of a uniform irrigation efficiency value does not capture local variations in irrigation performance, and spatial variations in RbIS should therefore be interpreted with this limitation in mind.

Moreover, RbIS for unauthorized irrigated areas was estimated by identifying irrigated croplands located outside the officially designated command areas or not registered within the irrigation scheme. Blue ET from these areas was aggregated to quantify total irrigation-related consumptive water use and then adjusted using the scheme-level irrigation efficiency to estimate the corresponding irrigation water abstraction.

2.3.6. Estimation of crop water requirements

Crop water requirements (ETc) were estimated for cotton and onion crops. Based on local agronomic information, cotton has a growing season of 165 days and is planted on 1 May, whereas onion has a growing season of 100 days and is planted on 1 August. ETc was estimated for each crop over its respective growing season.

Crop water requirements were calculated as follows:

$$ETc = Kc * ETo \tag{9}$$

Table 3
Summary of irrigation management scenarios evaluated to improve irrigation performance in the Amibara irrigation scheme.

Scenario	Description
Baseline	Represents the original baseline conditions, assuming no invasive tree species, a design irrigation efficiency of 49%, and a command area of 10,000 ha.
Scenario 1	Assumes improved irrigation efficiency and higher cropping intensity by shifting from furrow irrigation to sprinkler and drip irrigation systems. An irrigation efficiency of 75% is assumed for sprinkler systems (Howell, 2003) and 85% for drip systems (Keller and Bliesner, 2001; Burt et al., 1997).
Scenario 2	Assumes that the existing furrow irrigation system is upgraded by integrating low-cost soil moisture sensors, improving irrigation efficiency from the design value of 49–60% through better irrigation scheduling and reduced water losses (Pramanik et al., 2021).
Scenario 3	Assumes a mixed irrigation system combining furrow and sprinkler irrigation. In this scenario, 5000 ha are irrigated using improved furrow irrigation at 60% efficiency, and 5000 ha are irrigated using sprinkler irrigation at 80% efficiency with low-cost soil moisture sensors. This scenario improves water-use efficiency while reducing investment costs by upgrading existing furrow systems and gradually introducing sprinkler irrigation.

where, Kc is the crop coefficient, and ETo denotes the reference evapotranspiration determined from pan evaporation data obtained from Melka Werer Agricultural Research Center with a pan coefficient (Kp) of 0.75. This Kp value was locally calibrated by the Melka Werer Agricultural Research Center through comparison with FAO−56 Penman–Monteith estimates derived from available climatic observations. Seasonal crop water requirements were calculated by summing daily ETc values over the respective crop growing period.

2.3.7. *Irrigation performance indicators*

Several irrigation performance indicators have been developed to assess scheme performance by integrating remote sensing data with in situ observations (Chukalla et al., 2022). In this study, Equity, Relative Evapotranspiration (RET), and Relative Irrigation Supply (RIS) were selected as key indicators because they provide complementary insights into irrigation system performance by evaluating water distribution, crop water adequacy, and the balance between irrigation water supply and crop demand. These indicators were computed at block, canal, and scheme levels to capture the spatial variability in irrigation performance. Definitions, calculation formulas, and classification thresholds for each indicator are presented in Table 2.

Using these three performance indicators, irrigation performance was compared between 2010 and 2024. To ensure spatial comparability between the two years, the 2010 irrigation performance maps were masked using the 2024 cotton cultivation extent, thereby restricting the analysis to areas cultivated with cotton in 2024. This approach ensured that differences in irrigation performance reflected temporal changes rather than variations in the spatial extent of cultivated areas.

2.3.8. *Assessments of water management scenarios*

A scenario-based analysis was co-developed with the Ethiopian Ministry of Irrigation and Lowlands (MILLs) to support planning and decision-making for the Amibara Irrigation Scheme. The analysis evaluated alternative water management options to quantify potential water savings and identify opportunities to improve irrigation water use efficiency under existing hydrological and operational constraints.

Three scenarios were developed to estimate potential water savings from improved irrigation efficiency, and to assess whether the saved water could support expansion of the irrigated area (Table 3). The performance of each scenario was compared with the baseline condition to evaluate the effectiveness of the proposed management strategies. Across all scenarios, a consistent cropping pattern was assumed, with cotton cultivated during the main irrigation season (May–October) and onion during the secondary irrigation season (December–March). This cropping pattern was adopted based on the original scheme design document and the crop production priorities of MILLs.

The scenario analysis incorporated crop water requirements, water availability at the diversion weir, irrigation efficiency, the design intake

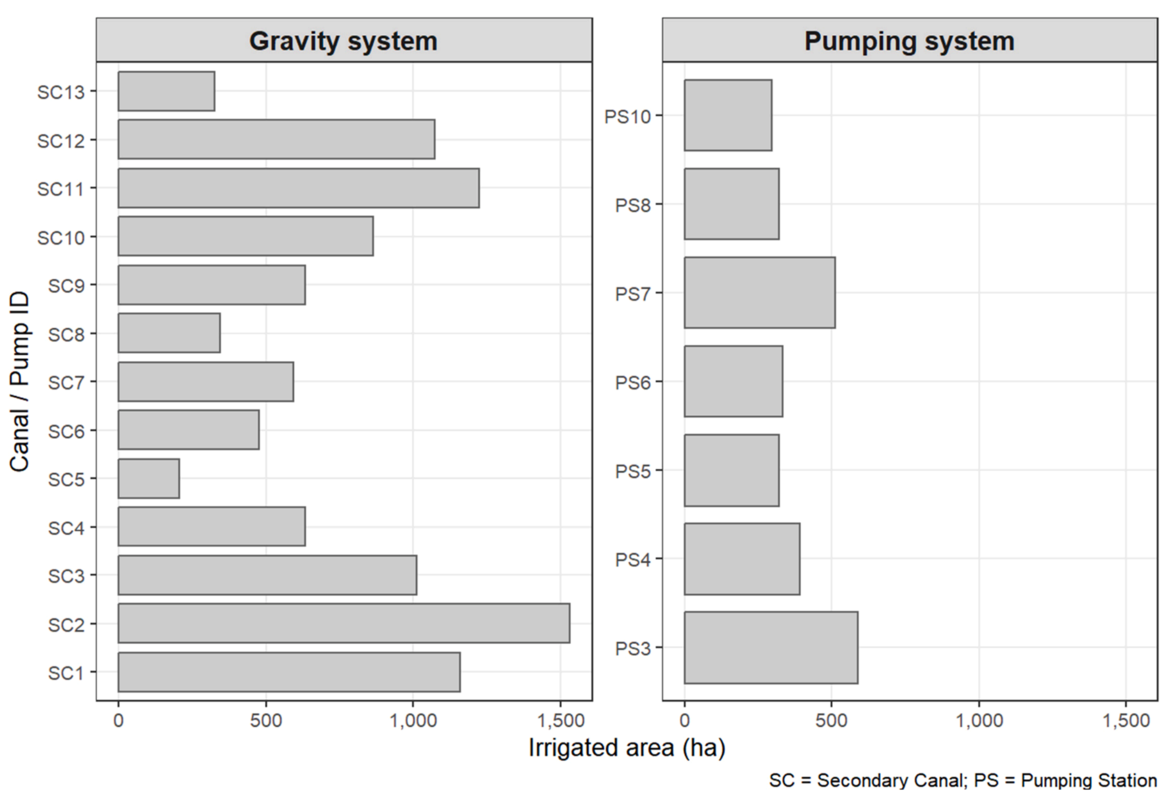

Fig. 3. Irrigated areas served by the gravity-fed canal network and pumping systems in the Amibara irrigation scheme.

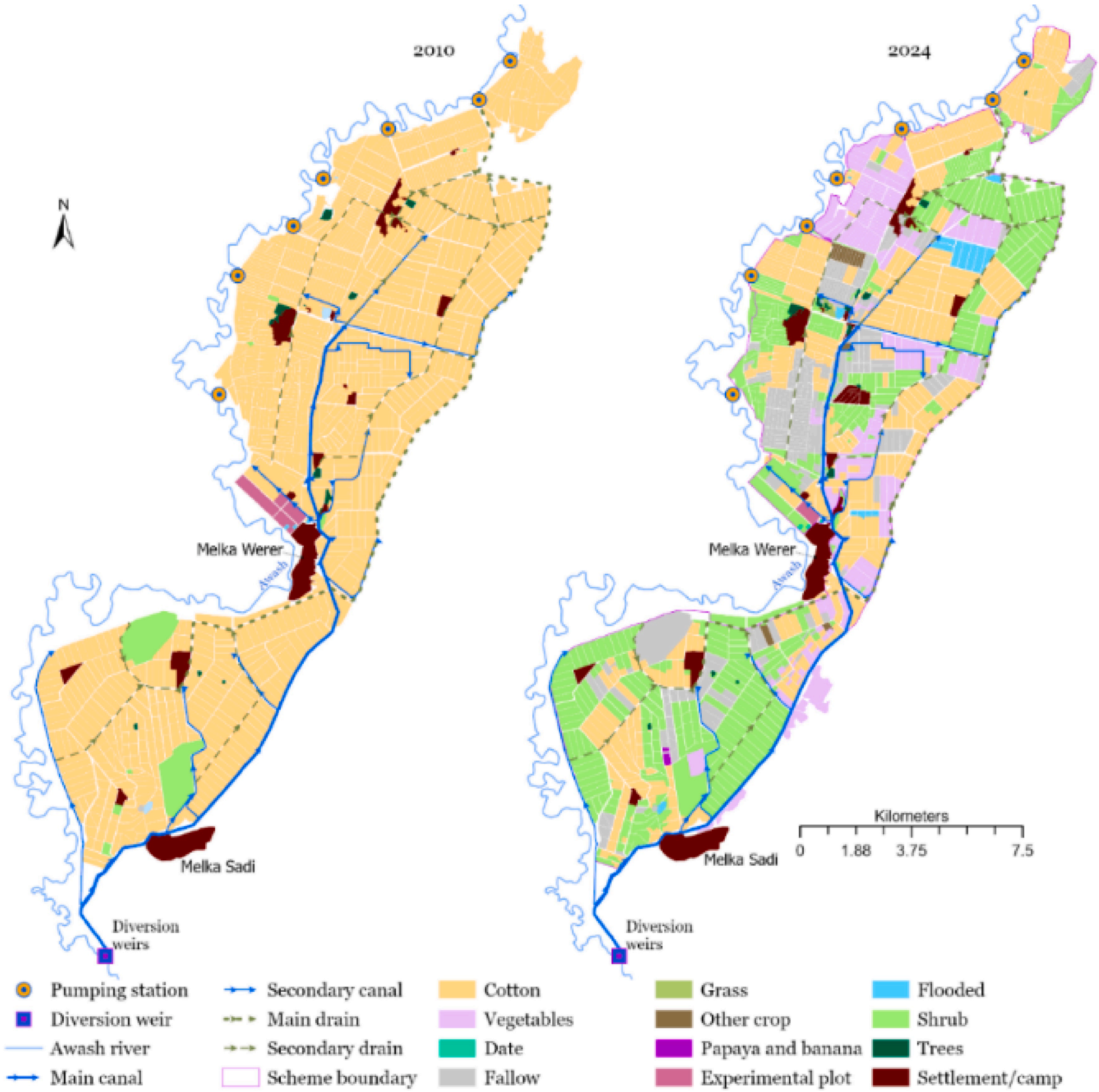

Fig. 4. Crop type maps for 2010 and 2024. Areas classified as shrubland are predominantly occupied by the invasive tree species, *Prosopis juliflora*.

capacity of the diversion weir, and downstream environmental flow requirements. Following Goshime et al. (2021), environmental flow requirements were defined as 20% of the long-term mean monthly flow and reserved to support downstream ecosystem needs. In all scenarios, water availability at the diversion site was represented by the 80% dependable flow derived from the flow-duration curve.

2.3.9. *Key informant interview and focus group discussion*

Key informant interviews (n = 16) and focus group discussions (three groups of seven participants each) were conducted in the study area, involving a total of 37 participants. To capture diverse perspectives across the irrigation scheme, participants were purposively selected from different locations within the scheme. Participants included representatives from the Amibara Irrigation farm enterprise, local smallholder farmers, irrigation investors managing leased land, officials from the Ministry of Irrigation and Lowlands, researchers from the Melka Werer Agricultural Research Center, and local government administrators. These engagements provided insights into the key challenges affecting irrigation water use and management, their underlying causes, and the operational practices influencing water distribution within the scheme. Information obtained from the key informant interviews and focus group discussions was subsequently used to interpret, validate, and complement the remote sensing–based estimates of irrigation water use, irrigation water supply, and irrigation performance.

3. Results and discussion

3.1. *Digitization of the scheme layout*

Digitization of the Amibara irrigation scheme identified

Table 4
Proportion of land cover types of Amibara irrigation scheme in 2010 and 2024. Irrigated areas under gravity and pumping irrigation systems are presented, with pumping system values indicated in brackets.

Class	LULC Type	2010		2024	
		Area in ha	%	Area in ha	%
Irrigated	Cotton	9747.5 (2850.6)	92.32	3165 (1324.7)	32.49
	Vegetables		-	1190(565)	12.71
	Research plot	187.6 (0)	1.37	31.3 (0)	0.23
	Date	5.9 (0)	0.04	6.6 (0)	0.05
	Banana	-	-	3.1 (0)	0.02
	Papaya	-	-	9.5 (0)	0.07
	Other crops	-	-	67.3 (33.6)	0.72
	Cotton flooded	-	-	59.4 (0)	0.43
Subtotal		9941 (2850.6)	93.73	4532 (1923.3)	46.71
Non irrigated	Shrubland	501.2	3.67	4866.4	35.21
	Fallow	-	-	2060.1	14.9
	Bare land saline	3.9	0.03	3.9	0.03
	Grass	-	-	20.5	0.15
	Trees	56.7	0.42	65.6	0.48
	Settlement	292.9	2.15	348.4	2.52
Subtotal		854.7	6.27	7364.9	53.28
Total		13,646.40	100	13,820.20	100

approximately 1306 irrigation blocks (Fig. 1). Of these, 451 blocks are supplied by pump-based systems that abstract water directly from the Awash River, while the remaining 855 blocks are served by a gravity-fed distribution network. The gravity system conveys water from the main canal through a hierarchical network consisting of 13 secondary canals and their associated tertiary canals.

Fig. 3 summarizes the command areas served by each secondary canal and pumping station. Among the secondary canals, SC2 has the largest irrigated area (1531 ha), followed by SC11 (1223 ha), whereas SC5 serves the smallest command area (204 ha). Within the pump-fed system, pumping stations 3 and 7 serve the largest irrigable areas. As the objective of this study was to evaluate the performance of the gravity-fed irrigation system, all subsequent analyses were restricted to the 855 blocks served by the gravity-fed canal network.

3.2. Crop type mapping

Crop type maps are presented in Fig. 4 and the corresponding area statistics are summarized in Table 4. In 2010, cotton was the overwhelmingly dominant crop, accounting for 92% of the total scheme area. By 2024, the cropping pattern had become more diversified, with cotton accounting for 33% of the scheme area and vegetables occupying approximately 13%. In addition, perennial crops such as banana (3 ha) and papaya (9.5 ha) were introduced, although they occupied only a small proportion of the scheme area.

Non-crop land cover types, particularly shrubland, expanded markedly from 3.7% (501 ha) in 2010 to 35.2% (4866 ha) in 2024. This expansion is largely attributed to farm abandonment, salinity buildup, and the rapid spread of *Prosopis juliflora*, which was further exacerbated by the 2020 flood. Fallow land also increased substantially, reaching 15% (2,060 ha) in 2024, thereby reducing the area available for crop production and potentially affecting overall agricultural output. Concurrently, the gravity-fed irrigated area declined from 9941 ha in 2010 to 4532 ha in 2024. In addition, about 160 ha of cultivated land was detected outside the official scheme boundary and was classified as unauthorized irrigated land.

3.3. Estimation and Validation of RbIS estimates

3.3.1. Validation using measured irrigation water supply data (2024)

Fig. 5 illustrates the spatial distribution of seasonal blue ET estimated across the Amibara irrigation scheme for 2010 and 2024. The results reveal notable changes in irrigation water consumption patterns over time, with mean seasonal blue ET decreased from 379 mm season^{-1} in 2010 to 342 mm season^{-1} in 2024.

The accuracy of the RbIS estimates was evaluated by comparing them with the measured irrigation water supply data collected from the experimental plot during the 2024/25 irrigation season (Fig. 6 right).

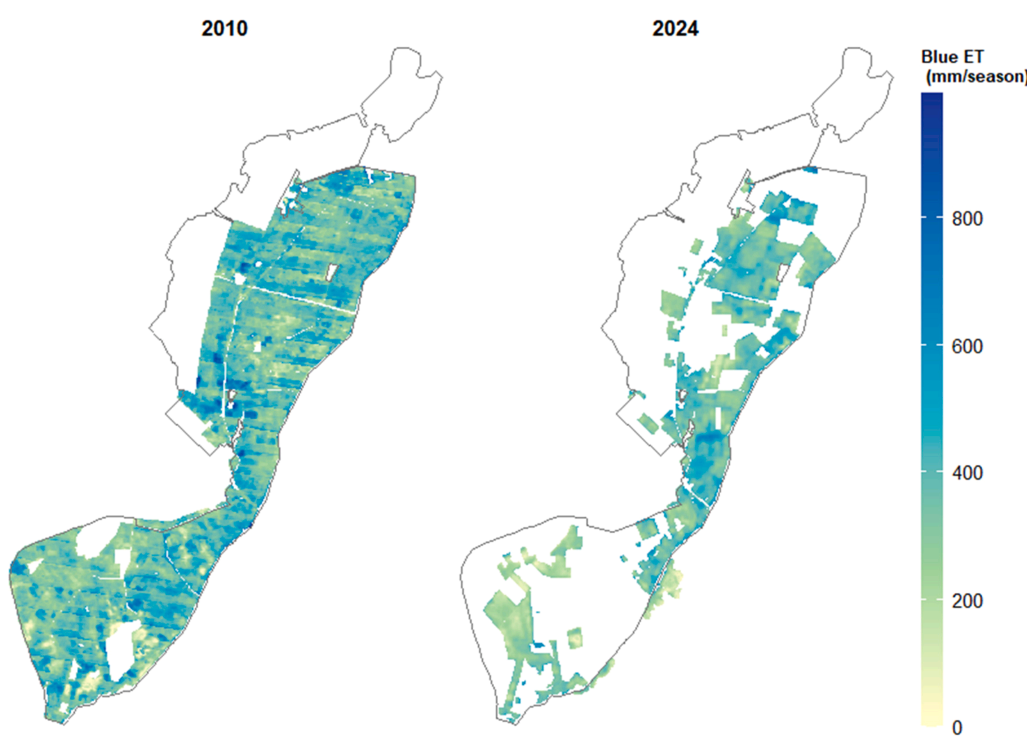

Fig. 5. Spatial distribution of seasonal Blue ET in the Amibara irrigation scheme for cotton in 2010, and for cotton and vegetable crops in 2024.

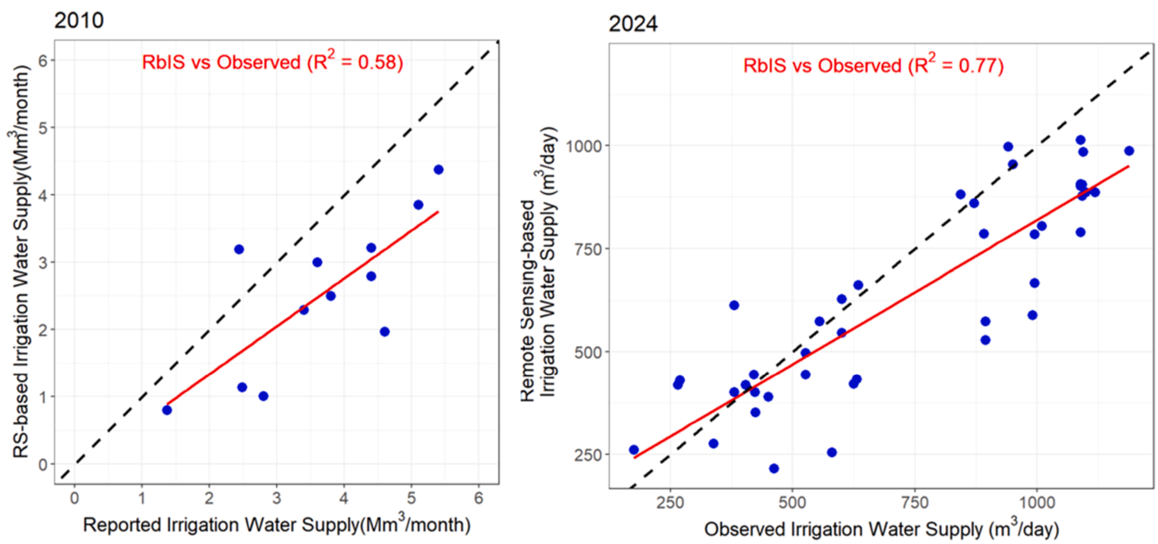

Fig. 6. Validation of remote sensing–based irrigation water supply (RbIS) estimates against observed irrigation water supply at canal (left) and field (right) scales. The left panel shows the comparison with reported canal-level irrigation supply data for 2010, while the right panel shows the comparison with measured irrigation supply at the experimental plot during the 2024/25 irrigation season. The dashed line indicates the 1:1 relationship and the red line indicates the fitted regression line.

The comparison showed strong agreement between estimated and observed irrigation water supply at the field scale ($R^2 = 0.77$, $p < 0.01$). For example, in January 2025, the measured irrigation supply was 11,651 m^3 $month^{-1}$, while the corresponding RbIS estimate was 9375 m^3 $month^{-1}$. Overall, the results demonstrate that the RbIS approach can reliably capture temporal variations in irrigation water supply.

3.3.2. Validation using historical irrigation water supply records (2010)

To further evaluate the reliability of the RbIS estimates, they were compared with reported canal-level irrigation water supply data for 2010 (Fig. 6). The results showed a moderate agreement between estimated and reported value ($R^2 = 0.58$). Bias analysis indicated that RbIS generally underestimated the reported irrigation supply. Similar discrepancies between remotely sensed and reported irrigation estimates have been reported in previous studies (Ji et al., 2025; Zipper et al., 2024). The observed differences may be attributed to uncertainties in remote sensing–derived evapotranspiration estimates (Mekonnen et al., 2022; Zhang et al., 2022; Zhu et al., 2022), assumptions regarding irrigation efficiency (Lankford, 2023), unaccounted conveyance and operational losses, and potential inaccuracies or inconsistencies in reported irrigation withdrawal data.

Interestingly, agreement between measured and estimated irrigation supply at the experimental plot (Fig. 6 right) was substantially stronger than that observed between reported and estimated irrigation supply in 2010 (Fig. 6 left). This suggests that part of the discrepancy may be associated with uncertainties in the reported irrigation supply data and the aggregation of water-use records across larger spatial units. Despite these limitations, the overall agreement between RbIS estimates and observed data indicates that the remote sensing–based approach can provide reliable estimates of irrigation water supply and support the monitoring and assessment of irrigation performance in data-scarce irrigation schemes.

3.4. Block-level irrigation performance assessment (2024)

Fig. 7 illustrates the spatial variability in irrigation performance across irrigation blocks for the 2024 irrigation season. Equity was generally moderate to good, with 57% of irrigation blocks classified as good equity, 37% fair equity, and only 6% poor equity. Nevertheless, irrigated areas with fair and poor equity remained evident, indicating persistent disparities in water distribution across the scheme.

The RIS maps show that irrigation deficits predominated across the scheme, with 63% of irrigation blocks receiving less water than required, compared with 5% classified as optimal and 32% as excess. Irrigation deficits were observed throughout the scheme and were not limited to downstream areas. Contrary to the commonly observed head–tail inequity in gravity-fed irrigation systems, where upstream users often secure preferential access to water (Janssen et al., 2011), several upstream blocks experienced severe irrigation deficits during 2024 season (Figs. 7 and 8). Field observations indicated that these deficits were primarily caused by infrastructure deterioration. Canal siltation and malfunctioning control gates reduced conveyance capacity and disrupted water delivery, even in areas located close to the diversion point. In contrast, several blocks in the middle and lower parts of the scheme received adequate or excessive irrigation water. This pattern suggests that irrigation outcomes were influenced more by infrastructure deterioration and operational failures than by systematic head–to–tail competition alone.

Findings from key informant interviews and focus group discussions corroborate the remote sensing–based assessment. Respondents consistently reported water shortages and intense competition to secure timely irrigation. They identified canal siltation, aging infrastructure, inadequate drainage maintenance, and excessive weed growth within the canal network as the primary underlying causes.

In terms of RET, irrigation performance was relatively better, with 42% of the irrigated area classified as acceptable and 33% as good, while 25% fell within the poor category (Fig. 7). By contrast, RIS indicated that irrigation deficits were widespread across the scheme. This contrast suggests that irrigation supply and crop water adequacy do not necessarily follow the same spatial patterns, highlighting the importance of assessing both indicators when evaluating irrigation performance. Similar discrepancies have been reported in previous studies (Levidow et al., 2014; Molle et al., 2016). These discrepancies may be associated with poor water distribution uniformity, suboptimal irrigation scheduling, soil-related limitations that restrict infiltration and root-zone water storage (Ferreira and Gonçalves, 2007; Gu et al., 2020; Priori et al., 2021), and inadequate field preparation, which can lead to highly variable within-field water distribution and localized waterlogging or deficits (Devkota et al., 2015). In addition, differences in the threshold values used to classify RET and RIS may partly explain some of the observed discrepancies.

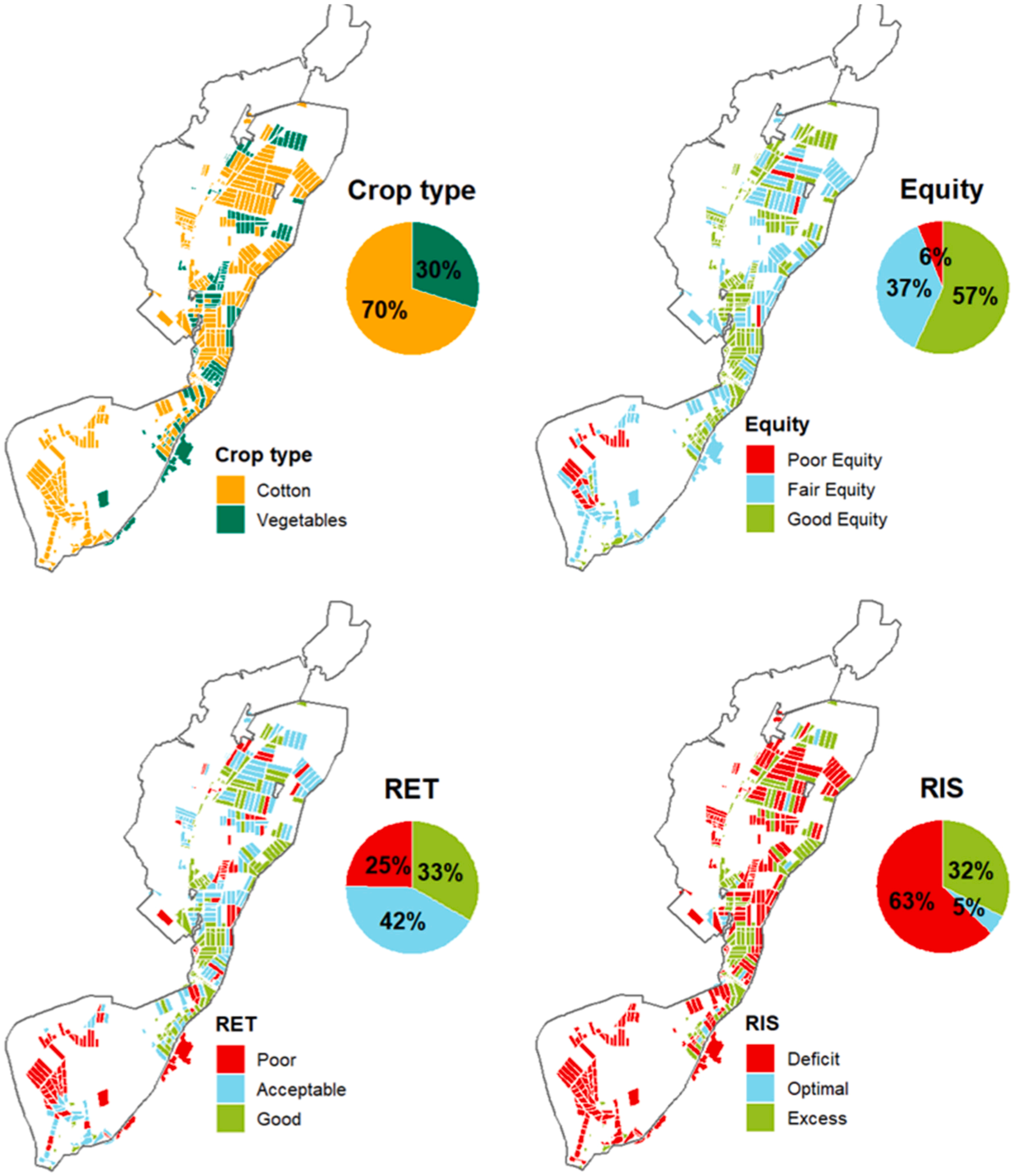

Fig. 7. Block-level Irrigation performance assessment for cotton (one season: May to October 15, 2024) and vegetables (August to November 5) under a gravity irrigation system. Water flows from south to north.

Table 5 further quantifies irrigation performance by crop type. Cotton covered 3165 ha, of which 23% was classified under poor RET and 40% as acceptable RET. In terms of irrigation supply, 26% of cotton blocks received excess irrigation relative to the seasonal net irrigation requirement of 720 mm. Vegetables occupied 1190 ha, with irrigation deficits affecting 40% of the area and acceptable RET observed in 51%. Excess irrigation occurred more frequently in vegetable blocks than in cotton blocks, indicating greater mismatches between irrigation supply and crop water requirements.

3.5. Comparison with historical block-level performance (2010)

Fig. 9 presents the spatial distribution of Equity, RET, and RIS across cotton irrigation blocks in 2010 and 2024, enabling a direct comparison of irrigation performance between the two years. Equity improved noticeably between the two years. In 2010, most irrigation blocks were classified as poor to fair (69%), with only a few localized areas exhibiting good equity (31%). By 2024, the proportion of blocks classified as fair and good increased (76%), indicating a more balanced distribution of irrigation water across the scheme. Although areas with poor equity persisted, suggesting that spatial disparities in water distribution remain an important management challenge in the scheme.

The spatial patterns of RET differ from those observed for RIS. In 2010, poor RET (60%) dominated much of the scheme, indicating that crop water requirements were not adequately met in many irrigation blocks. In 2024, a larger proportion of irrigation blocks fell within the acceptable and good RET (77%) categories, reflecting improvements in crop water consumption relative to crop water requirements.

In contrast, RIS revealed a substantial increase in irrigation deficits, with the proportion of cotton blocks experiencing deficit irrigation increasing from 40% in 2010 to 67% in 2024. In 2010, both deficit and excess irrigation were widespread, indicating considerable spatial variability in irrigation water supply across the scheme. Overall, these findings suggest that although water distribution became more equitable and crop water adequacy (RET) improved, the volume of irrigation water supplied relative to crop demand declined.

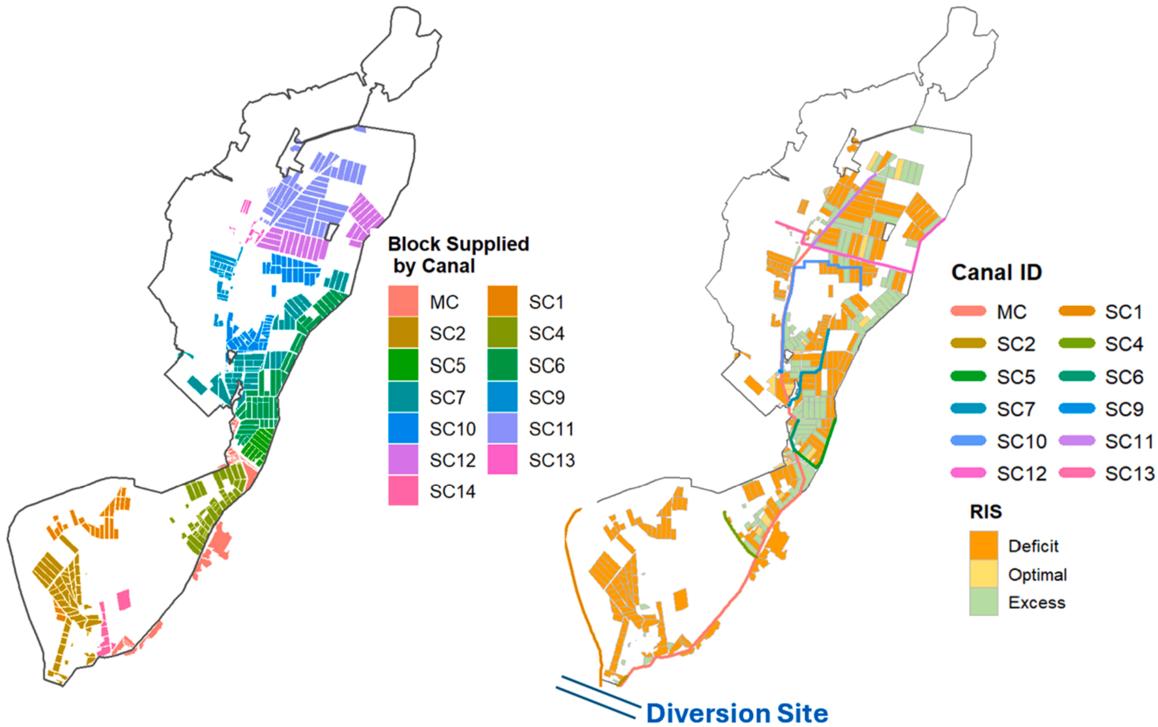

Fig. 8. Upstream irrigation blocks experienced water deficits due to siltation and malfunctioning gates. MC stands for main canal, and SC refers to secondary canal. Water flows from south to north.

Table 5
Distribution of cotton and vegetable crop areas across relative evapotranspiration (RET) and relative irrigation supply (RIS) performance classes for 2024.

RET (Cotton)		RIS (Cotton)		RET (Vegetable)		RIS (Vegetable)	
Class	Area (Ha)	Class	Area (Ha)	Class	Area (Ha)	Class	Area (Ha)
Poor	722	Deficit	2217	Poor	473	Deficit	719
Acceptable	1277	Optimal	142	Acceptable	602	Optimal	39
Good	1166	Excess	806	Good	115	Excess	432
Total	3165		3165		1190		1190

3.6. *Canal level irrigation performance assessment (2024)*

Considering the irrigation efficiency of the scheme, irrigation water supply at the canal level was tracked for 2024, and the results are presented in Fig. 10. The box plot reveals substantial variability in irrigation water supply among the canals, with notable differences in median values. On average, canal-level RIS was 0.8, indicating that irrigation water supply across the scheme was generally below crop water requirements. Most canals operated under deficit conditions, except for secondary canals 6, 10, and 13, which exhibited excess supply. Key informant interviews and focus group discussions with scheme operators and farmers corroborated these findings, highlighting persistent canal-level inefficiencies and uneven water distribution as major constraints on water availability across the command area.

Moreover, our results show that blocks served by secondary canals 1 and 2 experienced substantial irrigation deficits (Fig. 8). These shortages appear to be driven by two main factors. First, severe siltation within the canal network has reduced conveyance capacity and limited water distribution efficiency, as sediment deposition obstructs flow and lowers the volumes delivered to downstream blocks. Second, malfunctioning canal gates further exacerbate the problem by restricting water delivery. Both issues were observed during our field observations.

The RIS indicator further highlights issues of over- and under-irrigation supply relative to crop water requirements, reflecting varying levels of water stress or surplus across the system. Such spatial heterogeneity in irrigation performance is commonly observed in large-scale irrigation schemes, where uneven canal management and maintenance often result in inefficiencies and inequitable water distribution (Chukalla et al., 2022; Hashemy Shahdany et al., 2018; Ketsela et al., 2024; Wamala et al., 2023).

Table 6 shows the seasonal irrigation water supply delivered through the main canal (MC) and secondary canals (SC) for cotton (May–October) and Vegetable (August–November) crops. The irrigation water supply varied considerably among canals, ranging from 0.28 Mm^3 season^{-1} to 3.74 Mm^3 season^{-1} with a total irrigation supply of 28.5 Mm^3 season^{-1} . The total water supply (irrigation supply and effective rainfall) was estimated at 33.2 Mm^3 season^{-1} . Unauthorized abstraction from the main canal was estimated at 1.84 Mm^3 season^{-1} in 2024, irrigating 271 ha of which 160 ha of unauthorized cropland outside the scheme boundary and 111 ha within the scheme drawing water directly from the main canal without authorization.

3.7. *Impacts of alternative water management scenarios*

Before conducting the scenario analysis, water availability at the diversion site was assessed using the 80% dependable flow, and the results are presented in Fig. 11. The results show that the 80% dependable flow exceeded the design intake capacity of the diversion weir (13.2 m^3 s^{-1}), indicating that water availability at the diversion site is not a limiting factor for irrigation water supply in the scheme.

The potential water savings and opportunities for irrigated area expansion in the Amibara irrigation scheme under different

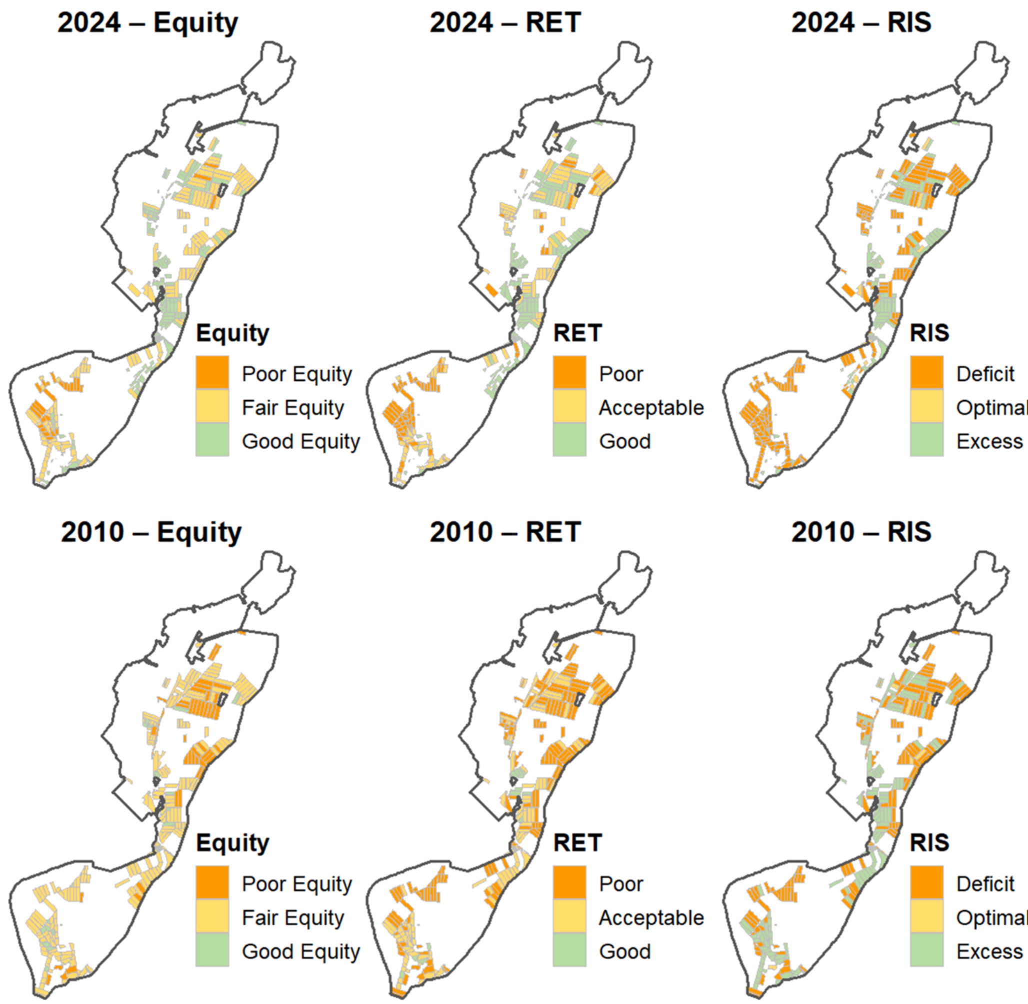

Fig. 9. Comparison of block-level irrigation performance for the cotton crop in 2010 and 2024. To ensure spatial comparability between the two years, the 2010 maps were masked to the 2024 cotton extent.

modernization scenarios are summarized in Table 7, while detailed calculations are provided in Annex 3.

Consistent with broader irrigation modernization evidence (FAO, 1997; Howell, 2003), the scenarios demonstrate that adopting improved irrigation technologies can substantially reduce water losses. Across the assessed interventions, total water savings range from 46 to 105 Mm^3 (Table 7), indicating considerable scope to enhance irrigation efficiency. These savings not only improve the internal performance of the scheme but also create opportunities to increase the irrigated area using the conserved water. In a basin where upstream abstractions are increasing, such as the Awash River Basin where the Amibara scheme is located, the conserved water could also serve as a strategic buffer to maintain reliable diversion flows at the weir site.

The scenario results reveal important differences in both water-saving potential and the level of technological investment required. Upgrading furrow irrigation with low-cost soil moisture sensors could save approximately 46 Mm^3 of water annually, while a hybrid furrow–sprinkler system could increase savings to 71 Mm^3 . Although the additional water savings are relatively small, both interventions offer opportunities to improve irrigation efficiency while utilizing much of the existing infrastructure. Such approaches may provide practical options for enhancing irrigation performance where large-scale modernization is financially or operationally challenging.

Converting the entire scheme to sprinkler irrigation could save 86 Mm^3 , while transitioning to drip irrigation, the most efficient system assessed, could save 105 Mm^3 . These findings align with the demonstrated efficiency benefits of pressurized irrigation systems (Howell, 2003). However, the greater water savings are accompanied by substantially higher investment costs, underscoring the need for careful cost–benefit and optimization analyses prior to large-scale implementation. The scenario comparisons therefore offer both a quantitative assessment of potential water savings and a practical basis for prioritizing interventions according to financial feasibility, management capacity, and long-term sustainability objectives.

More advanced pressurized irrigation systems, such as sprinkler and drip irrigation, are commonly associated with high application efficiencies (75–85%) under well-managed and properly maintained conditions (Howell, 2003; Van Halsema and Vincent 2012). However, the realization of such performance is strongly dependent on local agronomic and infrastructural conditions. In environments characterized by elevated sediment loads and salinity, as in the Amibara scheme, maintaining sprinkler nozzles and drip emitters at optimal performance can be challenging without adequate filtration systems, routine maintenance, and technical capacity. These requirements imply that the adoption of such systems would also entail substantial operational management and institutional support, in addition to the initial capital investment. Therefore, while these technologies represent a high-efficiency benchmark, their practical feasibility should be considered in the context of local biophysical constraints and long-term maintenance capacity

Beyond technological improvements, the analysis underscores the importance of addressing ecological pressures that constrain water

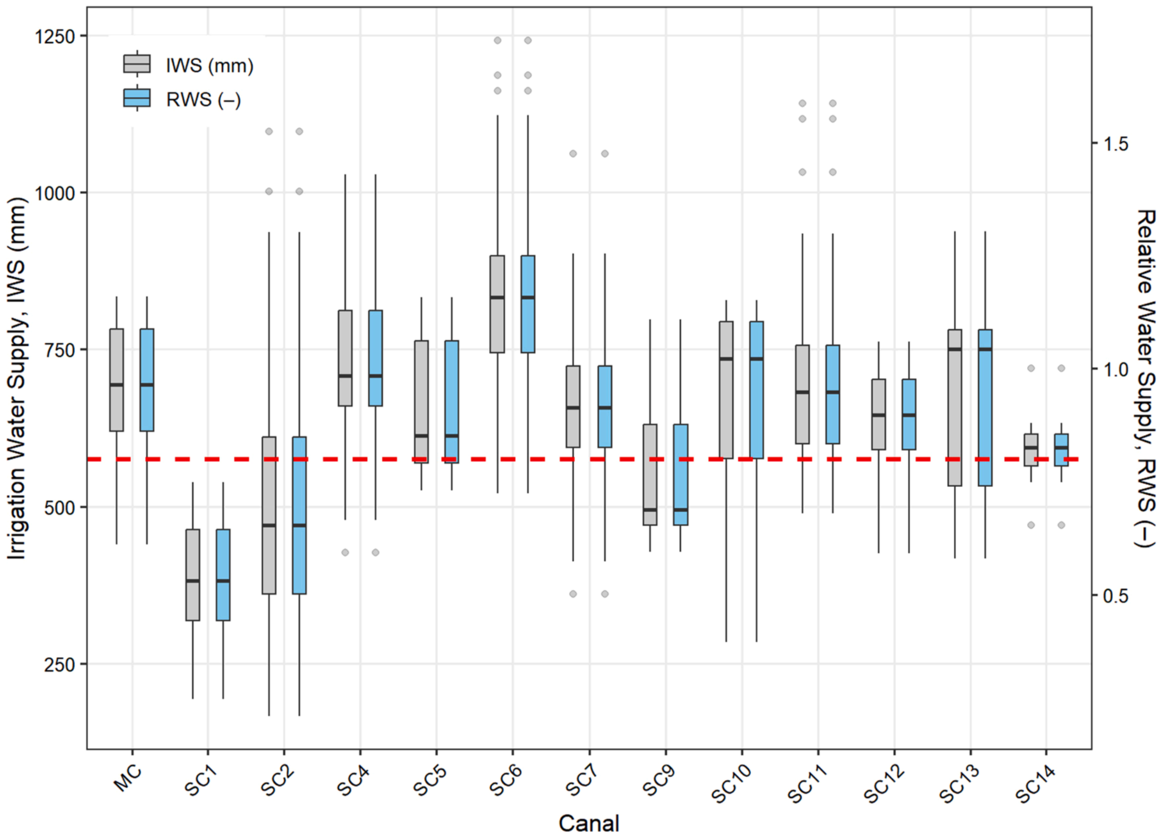

Fig. 10. Canal-level irrigation performance in 2024. For each canal, boxplots summarize the distribution of block-level values, where the box bounds represent the 25th and 75th percentiles and the central line indicates the median. In the top panel, the red dashed line indicates the mean seasonal irrigation supply (577 mm) relative to the net irrigation requirement for cotton (720 mm), and the corresponding mean relative irrigation supply (RIS = 0.8) compared with the optimal value (RIS = 1).

Table 6
Canal-level irrigation water supply estimated from remote sensing data for May–October 2024. Abbreviations: MC – main canal; SC – secondary canal; IS – irrigation supply; TWS – total water supply (IS plus effective rainfall).

Water Source	Area Served (Ha)	Water supply per season			
		IS (mm)	IS (Mm3)	TWS (mm)	TWS (Mm3)
MC	271.7	678.0	1.8	779.5	2.1
SC1	233.0	389.5	0.9	509.5	1.2
SC2	478.7	505.4	2.4	625.4	3.0
SC4	359.3	712.3	2.6	813.7	2.9
SC5	192.4	640.2	1.2	728.9	1.4
SC6	449.4	832.3	3.7	946.3	4.3
SC7	523.6	662.0	3.5	765.4	4.0
SC9	136.9	560.2	0.8	676.8	0.9
SC10	375.1	675.7	2.5	766.8	2.9
SC11	754.1	711.5	5.4	816.3	6.2
SC12	427.7	638.9	2.7	757.0	3.2
SC13	44.3	641.5	0.3	744.3	0.3
SC14	108.5	592.3	0.6	706.9	0.8
Total	4354.6	633.8	28.5	741.3	33.2

availability. The invasive tree species *Prosopis juliflora* continues to expand aggressively across the scheme, consuming significant amounts of water and encroaching onto productive farmland (Shiferaw et al., 2021). Its removal could release an additional 36 Mm^3 of water, complementing the gains achieved through irrigation modernization. Moreover, converting cleared biomass into bioenergy, charcoal, livestock feed, or construction materials presents an opportunity to offset removal costs while supporting local livelihoods. Integrating Prosopis management with irrigation modernization thus offers a dual pathway for enhancing water availability and promoting environmental and socioeconomic resilience within the scheme.

Together, these scenario-based findings provide a strong evidence base to guide MILLs in their revitalization efforts. They demonstrate not only the scale of potential water savings but also the trade-offs between cost, efficiency, and management complexity. Ultimately, prioritizing a balanced portfolio of interventions, combining ecological restoration, incremental efficiency improvements, and selective adoption of high-efficiency technologies will be essential for achieving long-term irrigation sustainability in the Amibara irrigation scheme.

3.8. Implications for agricultural water management

This study presents a multi-scale assessment framework that integrates high-spatial-resolution evapotranspiration estimates with water accounting to partition total evapotranspiration into blue and green components and estimate irrigation water supply in largely unmetered irrigation systems. By combining irrigation water supply estimates with irrigation performance indicators, the framework enables spatially explicit diagnosis of water use, water supply adequacy, and irrigation performance across multiple management scales.

The combined analysis of RET and RIS revealed substantial spatial variability in irrigation performance, with some canal command areas experiencing persistent water deficits while others received excess irrigation. Such information can help irrigation managers identify underperforming canals, prioritize maintenance and rehabilitation efforts, improve water delivery scheduling, and target interventions to areas where water shortages are most severe. The identification of unauthorized irrigated areas and the estimation of approximately 1.84 Mm^3 of unauthorized water withdrawals from the main canal further

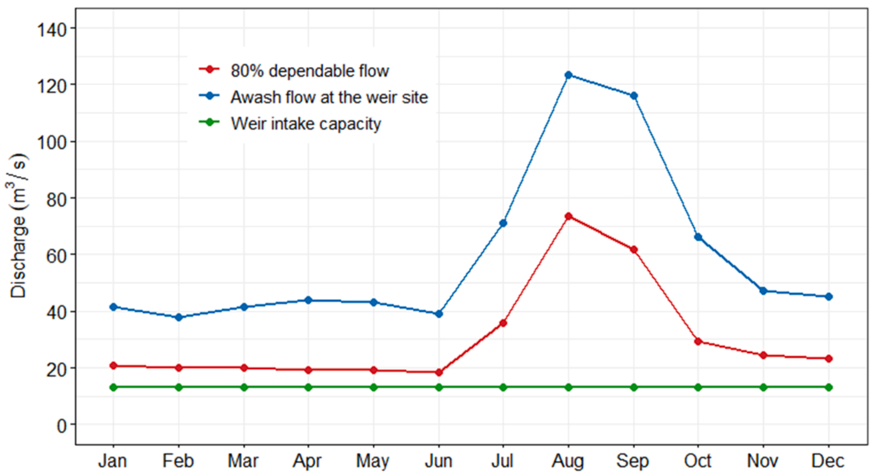

Fig. 11. Long-term average monthly flow at the weir site for the period 1991–2014.

Table 7
The volume of water that could be saved by different water management scenarios.

Scenarios	Water saved (Mm^3/yr)	Potential net increase in irrigated cropland (ha)*
Scenario 1 (Sprinkler)	86	17,200
Scenario 1 (Drip)	105	19,500
Scenario 2 (Furrow and low-cost soil moisture sensors)	46	13,700
Scenario 3 (Furrow and Sprinkler)	71	15,800

* Compared to the design irrigated area of 10,000 ha.

demonstrate the potential of the approach to support compliance monitoring and improve water allocation efficiency.

The scenario analysis highlights opportunities to improve water productivity through enhanced irrigation efficiency. For example, improving irrigation efficiency from the current level of approximately 32–60% through improved furrow irrigation management could save about 74 Mm^3 of water annually, while sprinkler and drip irrigation systems could generate even greater water savings. These savings could be used to expand irrigation to currently uncultivated areas, improve the reliability of water supply to existing users, or enhance environmental flow protection during periods of water scarcity. The results therefore provide quantitative evidence to support decisions on canal rehabilitation, irrigation modernization, and investments in improved on-farm water management technologies.

Beyond Amibara, the framework provides a practical approach for irrigation performance assessment in data-scarce regions where irrigation withdrawals are largely unmetered and flow-monitoring infrastructure is limited. By combining remotely sensed evapotranspiration, water accounting principles, and irrigation efficiency estimates, the methodology enables the estimation of irrigation water supply and the diagnosis of irrigation performance at multiple spatial scales. However, successful application requires supporting datasets, including crop type maps, irrigation network layouts, and representative irrigation efficiency estimates. As such datasets become increasingly available through remote sensing and digital water management initiatives, the framework has strong potential to support operational irrigation monitoring, water allocation planning, and evidence-based decision-making across large irrigation systems.

3.9. Limitations of the study

While the findings provide valuable insights into irrigation water management and rehabilitation planning in the Amibara Irrigation Scheme, the results should be interpreted within the context of the study assumptions and data availability. The estimation of RbIS relied on a representative scheme-wide irrigation efficiency parameter derived from field measurements of application efficiency and canal conveyance efficiency. Although this approach provides a practical basis for estimating irrigation water supply at the scheme scale, irrigation efficiency inevitably varies across the scheme because of differences in canal conditions, field management, and water delivery practices. Consequently, the spatial distribution of RbIS is influenced not only by spatial variations in blue evapotranspiration but also by the assumption of uniform irrigation efficiency. The identification of over- and under-supplied areas should therefore be interpreted as reflecting relative irrigation performance rather than precise field-scale estimates of irrigation supply.

The use of a representative scheme-wide irrigation efficiency parameter was necessary because irrigation withdrawals are largely unmetered and many flow-measurement structures within the scheme are non-functional, preventing the derivation of spatially distributed irrigation efficiencies. Future applications of the framework could further improve the estimation of irrigation water supply by incorporating spatially distributed irrigation efficiency values derived from additional field measurements or operational monitoring data as these become available.

The estimation of blue ET depends on remotely sensed evapotranspiration and the assumptions embedded within the soil moisture algorithm embedded in WA + , meaning that any uncertainty in these inputs directly affects the reliability of the derived blue ET and irrigation supply estimates. Although the evapotranspiration datasets and partitioning methodology showed reasonable agreement with field observations and reported irrigation supply data, uncertainties associated with evapotranspiration estimation, and gap-filling procedures may propagate into blue ET, and subsequently the derived irrigation water supply estimates. In addition, the use of a fixed pan coefficient to estimate ETo may introduce uncertainty into crop water requirement estimates, particularly under varying seasonal wind, humidity, and radiation conditions. Despite these assumptions and uncertainties, the integrated use of remote sensing, water accounting, field measurements, and irrigation performance indicators provides a robust framework for assessing irrigation water use and supply in data-scarce schemes.

4. Conclusion

This study presents a remote sensing–based approach to estimate irrigation water use and supply in the Amibara irrigation scheme for the years 2010 and 2024. High-resolution (30 m) Landsat-derived evapotranspiration data were integrated with the Water Accounting Plus (WA+) framework to partition the actual evapotranspiration into green and blue ET and derive RbIS. The approach was implemented at block, canal, and scheme scales using a digitized irrigation layout and crop type maps. Irrigation performance was subsequently evaluated at each scale using three indicators: Equity, RET, and RIS.

The good agreement between RbIS estimates and observed irrigation supply data demonstrates the potential of the proposed methodology for monitoring irrigation water supply in data-scarce irrigation schemes. The analysis indicates that irrigation performance in the Amibara Irrigation Scheme has declined considerably since 2010, with water deficits becoming more widespread and irrigation supply increasingly insufficient to meet crop water requirements. The coexistence of irrigation deficits, excess water applications, and unauthorized abstractions from the main canal highlights significant inefficiencies in water distribution and management. Addressing these inefficiencies through improved water allocation, infrastructure management, and monitoring of unauthorized withdrawals could substantially enhance scheme performance and water productivity. Overall, the methodology developed in this study provides a scalable and practical framework for irrigation monitoring in data-scarce schemes. Future studies would benefit from incorporating spatially distributed irrigation efficiency to improve the accuracy of remote sensing–based irrigation supply estimates.

CRediT authorship contribution statement

Kirubel Mekonnen: Writing – original draft, Visualization, Validation, Software, Methodology, Investigation, Formal analysis, Data curation, Conceptualization. **Mulugeta Tadesse:** Writing – review & editing, Validation, Methodology, Formal analysis, Data curation, Conceptualization. **Naga Manohar Velpuri:** Writing – review & editing, Supervision, Resources, Conceptualization. **Mohammed Abdella:** Writing – review & editing, Formal analysis, Data curation. **Mengistu Dessalegn:** Writing – review & editing, Data curation. **Mansoor Leh:** Writing – review & editing, Supervision, Conceptualization. **Komlavi Akpoti:** Writing – review & editing. **Afua Owusu:** Writing – review & editing. **Ashenafi Likessa:** Writing – review & editing, Data curation. **Abdulkarim Seid:** Writing – review & editing, Supervision, Resources, Project administration, Conceptualization.

Declaration of Competing Interest

The authors declare that they have no known competing financial interests or personal relationships that could have appeared to influence the work reported in this paper.

Acknowledgement

This research was undertaken as part of the International Water Management Institute's Digital Innovations for Water Secure Africa (DIWASA) project. We gratefully acknowledge the generous financial support of The Leona M and Harry B. Helmsley Charitable Trust.

Appendix A. Supporting information

Supplementary data associated with this article can be found in the online version at doi:10.1016/j.agwat.2026.110700.

Data Availability

Data will be made available on request.

References

Abera, A., Verhoest, N.E.C., Tilahun, S.A., Alamirew, T., Adgo, E., Moges, M.M., Nyssen, J., 2019. Performance of small-scale irrigation schemes in Lake Tana Basin of Ethiopia: technical and socio-political attributes. Phys. Geogr. 40 (3), 227–251. https://doi.org/10.1080/02723646.2018.1516445.

de Andrade, B.C.C., de Andrade Pinto, E.J., Ruhoff, A., Senay, G.B., 2021. Remote sensing-based actual evapotranspiration assessment in a data-scarce area of Brazil: A case study of the Urucuia Aquifer System. Int. J. Appl. Earth Obs. Geoinf. 98. https://doi.org/10.1016/j.jag.2021.102298.

Asres, S.B., 2016. Evaluating and enhancing irrigation water management in the upper Blue Nile basin, Ethiopia: The case of Koga large scale irrigation scheme. November 2015 Agric. Water Manag. 170, 26–35. https://doi.org/10.1016/j.agwat.2015.10.025.

Bashe, T., Alamirew, T., Dejen, Z.A., 2023. Evaluating Performance of Community-based Irrigation Schemes Using Remote-sensing Technologies to Enhance Sustainable Irrigation Water Management. Water Conserv. Sci. Eng. 8 (1). https://doi.org/10.1007/s41101-023-00222-y.

Burt, C.M., Clemmens, A.J., Strelkoff, T.S., Solomon, K.H., Bliesner, R.D., Hardy, L.A., Howell, T.A., Eisenhauer, D.E., 1997. Irrigation Performance Measures: Efficiency and Uniformity. J. Irrig. Drain. Eng. 123 (6), 423–442.

Chukalla, A.D., Mul, M.L., Van Der Zaag, P., Van Halsema, G., Mubaya, E., Muchanga, E., Den Besten, N., Karimi, P., 2022. A framework for irrigation performance assessment using WaPOR data: The case of a sugarcane estate in Mozambique. Hydrol. Earth Syst. Sci. 26 (10), 2759–2778. https://doi.org/10.5194/hess-26-2759-2022.

De Boer, F., 2016. HiHydroSoil: a High Resolution Soil Map of Hydraulic Properties (Version 1.2). Report. Future 134.

Dembélé, M., Salvadore, E., Zwart, S., Ceperley, N., Mariéthoz, G., Schaefli, B., 2023. Water accounting under climate change in the transboundary Volta River Basin with a spatially calibrated hydrological model. J. Hydrol. 626 (6). https://doi.org/10.1016/j.jhydrol.2023.130092.

Devkota, K.P., Hoogenboom, G., Boote, K.J., Singh, U., Lamers, J.P.A., Devkota, M., Vlek, P.L.G., 2015. Simulating the impact of water saving irrigation and conservation agriculture practices for rice-wheat systems in the irrigated semi-arid drylands of Central Asia. Agric. For. Meteorol. 214 (215), 266–280. https://doi.org/10.1016/j.agrformet.2015.08.264.

Dile, Y.T., Ayana, E.K., Worqlul, A.W., Xie, H., Srinivasan, R., Lefore, N., You, L., Clarke, N., 2020. Evaluating satellite-based evapotranspiration estimates for hydrological applications in data-scarce regions: A case in Ethiopia. Sci. Total. Environ. 743, 140702. https://doi.org/10.1016/j.scitotenv.2020.140702.

van Eekelen, M.W., Bastiaanssen, W.G.M., Jarmain, C., Jackson, B., Ferreira, F., van der Zaag, P., Saraiva Okello, A., Bosch, J., Dye, P., Bastidas-Obando, E., Dost, R.J.J., Luxemburg, W.M.J., 2015. A novel approach to estimate direct and indirect water withdrawals from satellite measurements: A case study from the Incomati basin. Agric. Ecosyst. Environ. 200, 126–142. https://doi.org/10.1016/j.agee.2014.10.023.

FAO, 1997. Modernization of Irrigation Schemes: Past Experiences and Future Options. Food and Agriculture Organization of the United Nations (Bangkok).

FAO, 2020. WaPOR evapotranspiration (ET) dataset. Food and Agriculture Organization of the United Nations (1989). Irrigation water management: Irrigation system performance. FAO Irrigation and Drainage Paper, p. 40. https://wapor.apps.fao.orgFAO (1989).

Ferreira, T.C., Gonçalves, D.A., 2007. Crop-yield/water-use production functions of potatoes (Solanum tuberosum, L.) grown under differential nitrogen and irrigation treatments in a hot, dry climate. Agric. Water Manag. 90 (1–2), 45–55. https://doi.org/10.1016/j.agwat.2007.02.012.

Foster, T., Mieno, T., Brozović, N., 2020. Satellite-Based Monitoring of Irrigation Water Use: Assessing Measurement Errors and Their Implications for Agricultural Water Management Policy. Water Resour. Res. 56 (11). https://doi.org/10.1029/2020WR028378.

Funk, C., Peterson, P., Landsfeld, M., Pedreros, D., Verdin, J., Shukla, S., Husak, G., Rowland, J., Harrison, L., Hoell, A., Michaelsen, J., 2015. The climate hazards infrared precipitation with stations - A new environmental record for monitoring extremes. Sci. Data 2, 1–21. https://doi.org/10.1038/sdata.2015.66.

Goshime, D.W., Haile, A.T., Rientjes, T., Absi, R., Ledésert, B., Siegfried, T., 2021. Implications of water abstraction on the interconnected Central Rift Valley Lakes sub-basin of Ethiopia using WEAP. J. Hydrol. Reg. Stud. 38, 100969. https://doi.org/10.1016/j.ejrh.2021.100969.

Gu, Z., Qi, Z., Burghate, R., Yuan, S., Jiao, X., Xu, J., 2020. Irrigation Scheduling Approaches and Applications: A Review. J. Irrig. Drain. Eng. 146 (6). https://doi.org/10.1061/(asce)ir.1943-4774.0001464.

Haj-Amor, Z., Ritzema, H., Hashemi, H., Bouri, S., 2018. Surface irrigation performance of date palms under water scarcity in arid irrigated lands. Arab. J. Geosci. 11, 27. https://doi.org/10.1007/s12517-017-3374-5.

Halcrow, 1983. Amibara Irrigation Project — Water Management Manual. Prepared for the Water Resources Development Authority. Government of Ethiopia. July 1983.

Hashemy Shahdany, S.M., Firoozfar, A., Maestre, J.M., Mallakpour, I., Taghvaeian, S., Karimi, P., 2018. Operational performance improvements in irrigation canals to overcome groundwater overexploitation (April). Agric. Water Manag. 204, 234–246. https://doi.org/10.1016/j.agwat.2018.04.014.

Howell, T.A., 2003. Irrigation Efficiency. Encyclopedia of Water Science. Marcel Dekker, New York.

Janssen, M.A., Anderies, J.M., Cardenas, J.C., 2011. Head-enders as stationary bandits in asymmetric commons: Comparing irrigation experiments in the laboratory and the field. Ecol. Econ. 70 (9), 1590–1598. https://doi.org/10.1016/j.ecolecon.2011.01.006.

Ji, L., Senay, G.B., Friedrichs, M., Kagone, S., 2025. Estimating agricultural irrigation water consumption for the High Plains aquifer region with integrated energy- and water-balance evapotranspiration modeling approaches. Agric. Water Manag. 309 (January), 109308. https://doi.org/10.1016/j.agwat.2025.109308.

Karimi, P., Bastiaanssen, W.G.M., Molden, D., 2013. Water Accounting Plus (WA+) - A water accounting procedure for complex river basins based on satellite measurements. Hydrol. Earth Syst. Sci. 17 (7), 2459–2472. https://doi.org/10.5194/hess-17-2459-2013.
Karimi, P., Bongani, B., Blatchford, M., de Fraiture, C., 2019. Global satellite-based ET products for the local level irrigation management: An application of irrigation performance assessment in the Sugarbelt of Swaziland. Remote. Sens. 11 (6). https://doi.org/10.3390/rs11060705.
Keller, J., Bliesner, R.D., 2001. Sprinkle and trickle irrigation. Blackburn Press, Caldwell, NJ.
Ketsela, Y.S., Reta, B.G., Muche, A.T., 2024. Evaluation of Small-Scale Irrigation Scheme Performance and Proposed Alternative Mitigation for Improved Water Management on Wezeqa and Gatto Irrigation Schemes, Southern, Ethiopia. Adv. Agric. 2024 (1). https://doi.org/10.1155/2024/5884209.
Lankford, B.A., 2023. Resolving the paradoxes of irrigation efficiency: Irrigated systems accounting analyses depletion-based water conservation for reallocation. April 2022 Agric. Water Manag. 287, 108437. https://doi.org/10.1016/j.agwat.2023.108437.
Levidow, L., Zaccaria, D., Maia, R., Vivas, E., Todorovic, M., Scardigno, A., 2014. Improving water-efficient irrigation: Prospects and difficulties of innovative practices. Agric. Water Manag. 146, 84–94. https://doi.org/10.1016/j.agwat.2014.07.012.
Mekonnen, Y.G., Alamirew, T., Tadesse, K.B., Chukalla, A.D., 2024. Monitoring small-scale irrigation performance using remote sensing in the Upper Blue Nile Basin, Ethiopia. Agric. Water Manag. 300 (June), 108928. https://doi.org/10.1016/j.agwat.2024.108928.
Mekonnen, K., Melesse, A.M., Woldesenbet, T.A., 2022. How suitable are satellite rainfall estimates in simulating high flows and actual evapotranspiration in MelkaKunitre catchment, Upper Awash Basin, Ethiopia? Sci. Total. Environ. 806, 150443. https://doi.org/10.1016/j.scitotenv.2021.150443.
Mekonnen, K., Velpuri, N.M., Leh, M., Akpoti, K., Owusu, A., Tinonetsana, P., Hamouda, T., Ghansah, B., Paranamana, T.P., Munzimi, Y., 2023. Accuracy of satellite and reanalysis rainfall estimates over Africa: A multi-scale assessment of eight products for continental applications. J. Hydrol. Reg. Stud. 49 (April), 101514. https://doi.org/10.1016/j.ejrh.2023.101514.
Mekonnen, K., Velpuri, N.M., Leh, M., Akpoti, K., Owusu, A., Mahapatra, S., Tinonetsana, P., Madushanka, L., Perera, T., Tedla, H.Z., Talema, M., Seid, A., 2026. An integrated modeling framework for water accounting assessment in the Lake Tana Sub-Basin, Ethiopia: Impacts of interbasin water transfer. J. Hydrol. Reg. Stud. 65, 103318. https://doi.org/10.1016/j.ejrh.2026.103318.
Miralles, D.G., De Jeu, R.A.M., Gash, J.H., Holmes, T.R.H., Dolman, A.J., 2011. Magnitude and variability of land evaporation and its components at the global scale. Hydrol. Earth Syst. Sci. 15 (3), 967–981. https://doi.org/10.5194/hess-15-967-2011.
Molle, F., Gaafar, I.A., El-agha, D.E., Rap, E., 2016. Irrigation Efficiency and the Nile Delta Water Balance. Water Salt Manag. Nile Delta. Report. 9 (December).
Mu, Q., Zhao, M., Running, S.W., 2011. Improvements to a MODIS global terrestrial evapotranspiration algorithm. Remote. Sens. Environ. 115 (8), 1781–1800. https://doi.org/10.1016/j.rse.2011.02.019.
Muturi, J.W., Ndehedehe, C.E., Kennard, M.J., 2025. A review of the use of remote sensing techniques in assessing irrigation water use. Agric. Water Manag. 319 (May), 109759. https://doi.org/10.1016/j.agwat.2025.109759.
Myneni, R.B., Hoffman, S., Knyazikhin, Y., Privette, J.L., Glassy, J., Tian, Y., Wang, Y., Song, X., Zhang, Y., Smith, G.R., Lotsch, A., Friedl, M., Morisette, J.T., Votava, P., Nemani, R.R., Running, S.W., 2002. Global products of vegetation leaf area and fraction absorbed PAR from year one of MODIS data. Remote. Sens. Environ. https://doi.org/10.1016/S0034-4257(02)00074-3.
Nasta, P., Franz, T.E., Gibson, J.P., Romano, N., 2023. Revisiting the definition of field capacity as a functional parameter in a layered agronomic soil profile beneath irrigated maize. Agric. Water Manag. 284, 108368. https://doi.org/10.1016/j.agwat.2023.108368.
OECD, 2015. Drying wells, rising stakes: Towards sustainable agricultural groundwater use. OECD Publishing, Paris, France.
Owusu, A., Kagone, S., Leh, M., Velpuri, N.M., Gumma, M.K., Ghansah, B., Thilina-Prabhath, P., Akpoti, K., Mekonnen, K., Tinonetsana, P., Mohammed, I., 2024. A framework for disaggregating remote-sensing cropland into rainfed and irrigated classes at continental scale. Int. J. Appl. Earth Obs. Geoinf. 126 (ember 2023), 103607. https://doi.org/10.1016/j.jag.2023.103607.
Poudel, U., Stephen, H., Ahmad, S., 2021. Evaluating irrigation performance and water productivity using eeflux et and ndvi. Sustain. (Switz.) 13 (14). https://doi.org/10.3390/su13147967.
Pramanik, M., Khanna, M., Singh, M., Singh, D., Sudhishri, S., Bhatia, A., Ranjan, R., 2021. Automation of soil moisture sensor-based basin irrigation system. Smart Agric. Technol. 2, 100032. https://doi.org/10.1016/j.atech.2021.100032.
Priori, S., Pellegrini, S., Vignozzi, N., Costantini, E.A.C., 2021. Soil Physical-Hydrological Degradation in the Root-Zone of Tree Crops: Problems and Solutions. Agronomy 11 (1). https://doi.org/10.3390/agronomy11010068.
Rinaudo, J.-D., Moreau, C., Garin, P., 2016. Social justice and groundwater allocation in agriculture: A French case study, Integrated groundwater management. Springer, Cham, pp. 273–293.
Sahle, G.T., 2009. Masters thesis, Addis Ababa University. Surf. Water Groundw. Interact. Eff. Irrig. Water Soil. Resour. Awash Val.
Senay, G.B., Bohms, S., Singh, R.K., Gowda, P.H., Velpuri, N.M., Alemu, H., Verdin, J.P., 2013. Operational evapotranspiration mapping using remote sensing and weather datasets: A new parameterization for the SSEB approach. J. Am. Water Resour. Assoc. 49 (3), 577–591. https://doi.org/10.1111/jawr.12057.
Senay, G.B., Friedrichs, M., Morton, C., Parrish, G.E., Schauer, M., Khand, K., Huntington, J., 2022. Mapping actual evapotranspiration using Landsat for the conterminous United States: Google Earth Engine implementation and assessment of the SSEBop model. Remote. Sens. Environ. 275, 113011.
Senay, G.B., Friedrichs, M., Singh, R.K., Velpuri, N.M., 2016. Evaluating Landsat 8 evapotranspiration for water use mapping in the Colorado River Basin. Remote. Sens. Environ. 185, 171–185. https://doi.org/10.1016/j.rse.2015.12.043.
Senay, G.B., Kagone, S., Velpuri, N.M., 2020. Operational global actual evapotranspiration: Development, evaluation, and dissemination. Sens. (Switz.) 20 (7), 1–18. https://doi.org/10.3390/s20071915.
Senkondo, W., Munishi, S.E., Tumbo, M., Nobert, J., Lyon, S.W., 2019. Comparing remotely-sensed surface energy balance evapotranspiration estimates in heterogeneous and data-limited regions: A case study of Tanzania's Kilombero Valley. Remote. Sens. 11 (11). https://doi.org/10.3390/rs11111289.
Shiferaw, W., Demissew, S., Bekele, T., Aynekulu, E., Pitroff, W., 2021. Invasion of Prosopis juliflora and its effects on soil physicochemical properties in Afar region, Northeast Ethiopia. Int. Soil. Water Conserv. Res. 9 (4), 631–638. https://doi.org/10.1016/j.iswcr.2021.04.003.
Siabi, N., Sanaeinejad, S.H., Ghahraman, B., 2022. Effective method for filling gaps in time series of environmental remote sensing data: An example on evapotranspiration and land surface temperature images. Comput. Electron. Agric. 193, 106619. https://doi.org/10.1016/j.compag.2021.106619.
Simons, G., Koster, R., Droogers, P., 2020. HiHydroSoil v2. 0 - High. Resolut. Soil. Maps Glob. Hydraul. Prop.
Tran, B.N., Van Der Kwast, J., Seyoum, S., Uijlenhoet, R., Jewitt, G., Mul, M., 2023. Uncertainty assessment of satellite remote-sensing-based evapotranspiration estimates: a systematic review of methods and gaps. Hydrol. Earth Syst. Sci. 27 (24), 4505–4528. https://doi.org/10.5194/hess-27-4505-2023.
Usman, M., Mahmood, T., Conrad, C., Bodla, H.U., 2020. Remote sensing and modelling based framework for valuing irrigation system efficiency and steering indicators of consumptive water use in an irrigated region. Sustain. (Switz.) 12 (22), 1–35. https://doi.org/10.3390/su12229535.
Van Halsema, G.E., Vincent, L., 2012. Efficiency and productivity terms for water management: A matter of contextual relativism versus general absolutism. Agric. Water Manag. 108, 9–15. https://doi.org/10.1016/j.agwat.2011.05.016.
Velpuri, N.M., Senay, G.B., 2017. Partitioning Evapotranspiration into Green and Blue Water Sources in the Conterminous United States. Sci. Rep. https://doi.org/10.1038/s41598-017-06359-w.
Wamala, F., Gidudu, A., Wanyama, J., Nakawuka, P., Bwambale, E., Chukalla, A.D., 2023. Assessment of irrigation water distribution using remotely sensed indicators: A case study of Doho Rice Irrigation Scheme, Uganda. Smart Agric. Technol. 4 (January), 100184. https://doi.org/10.1016/j.atech.2023.100184.
Wang, Q., Wang, L., Zhu, X., Ge, Y., Tong, X., Atkinson, P.M., 2022. Remote sensing image gap filling based on spatial-spectral random forests (April). Sci. Remote. Sens. 5, 100048. https://doi.org/10.1016/j.srs.2022.100048.
World Bank, 1990. Project Completion Report. Report No. 8708. In: Revised Amibara Irrigation Project. The World Bank, Washington DC.
Yadeta, B., Ayana, M., Yitayew, M., Hordofa, T., 2022. Performance evaluation of furrow irrigation water management practice under Wonji Shoa Sugar Estate condition, in Central Ethiopia. J. Eng. Appl. Sci. 69 (1), 1–23. https://doi.org/10.1186/s44147-022-00071-x.
Zeray, N., Legesse, B., Mohamed, J.H., Aredo, M.K., 2017. Impacts of Prosopis juliflora invasion on livelihoods of pastoral and agro-pastoral households of Dire Dawa Administration, Ethiopia. Pastoralism 7 (1). https://doi.org/10.1186/s13570-017-0079-z.
Zhang, K., Li, X., Zheng, D., Zhang, L., Zhu, G., 2022. Estimation of Global Irrigation Water Use by the Integration of Multiple Satellite Observations. Water Resour. Res. 58 (3), 1–23. https://doi.org/10.1029/2021WR030031.
Zhao, M., Heinsch, F.A., Nemani, R.R., Running, S.W., 2005. Improvements of the MODIS terrestrial gross and net primary production global data set. Remote. Sens. Environ. https://doi.org/10.1016/j.rse.2004.12.011.
Zhu, W., Tian, S., Wei, J., Jia, S., Song, Z., 2022. Multi-scale evaluation of global evapotranspiration products derived from remote sensing images: Accuracy and uncertainty (January). J. Hydrol. 611, 127982. https://doi.org/10.1016/j.jhydrol.2022.127982.
Zipper, S., Kastens, J., Foster, T., Wilson, B.B., Melton, F., Grinstead, A., Deines, J.M., Butler, J.J., Marston, L.T., 2024. Estimating irrigation water use from remotely sensed evapotranspiration data: Accuracy and uncertainties at field, water right, and regional scales (July). Agric. Water Manag. 303, 109036. https://doi.org/10.1016/j.agwat.2024.109036.
Zwart, S.J., Leclert, L.M.C., 2010. A remote sensing-based irrigation performance assessment: A case study of the Office du Niger in Mali. Irrig. Sci. 28 (5), 371–385. https://doi.org/10.1007/s00271-009-0199-3.